

PB 181508

Price \$1.75

**AN INVESTIGATION OF MIDSHIP BENDING MOMENTS  
EXPERIENCED IN EXTREME REGULAR WAVES BY MODELS  
OF THE MARINER TYPE SHIP AND THREE VARIANTS**

**SSC-155**

**By  
J. F. DALZELL**

**SHIP STRUCTURE COMMITTEE**

For sale by the U.S. Department of Commerce, Office of Technical Services,  
Washington, D.C., 20230

# SHIP STRUCTURE COMMITTEE

## MEMBER AGENCIES:

BUREAU OF SHIPS, DEPT. OF NAVY  
MILITARY SEA TRANSPORTATION SERVICE, DEPT. OF NAVY  
UNITED STATES COAST GUARD, TREASURY DEPT.  
MARITIME ADMINISTRATION, DEPT. OF COMMERCE  
AMERICAN BUREAU OF SHIPPING

## ADDRESS CORRESPONDENCE TO:

SECRETARY  
SHIP STRUCTURE COMMITTEE  
U. S. COAST GUARD HEADQUARTERS  
WASHINGTON 25, D. C.

January 15, 1964

Dear Sir:

The Ship Structure Committee has sponsored a research project at Stevens Institute of Technology entitled "Model in Extreme Waves." The purpose of the project was to determine the upper limit of longitudinal seaway bending moments by direct measurement on ship models in tank waves of maximum steepness, supplemented by theoretical calculations.

Herewith is a copy of the First Progress Report, SSC-155 An Investigation of Midship Bending Moments Experienced in Extreme Regular Waves by Models of the Mariner Type Ship and Three Variants by J. F. Dalzell.

The project was conducted under the advisory guidance of the Committee on Ship Structural Design of the National Academy of Sciences-National Research Council.

Comments on this report would be welcomed and should be addressed to the Secretary, Ship Structure Committee.

Yours sincerely,



T. J. FABIK  
Rear Admiral, U. S. Coast Guard  
Chairman, Ship Structure  
Committee

SSC-155

First Progress Report  
of  
Project SR-157  
"Model in Extreme Waves"

to the

Ship Structure Committee

AN INVESTIGATION OF MIDSHIP BENDING MOMENTS  
EXPERIENCED IN EXTREME REGULAR WAVES BY MODELS OF THE  
MARINER TYPE SHIP AND THREE VARIANTS

by

J. F. Dalzell

Stevens Institute of Technology

under

Department of the Navy  
Bureau of Ships Contract NObs-78211

Washington, D. C.  
U. S. Department of Commerce, Office of Technical Services  
January 15, 1964

## ABSTRACT

This report summarizes experimental research to investigate the possibility of a physical upper limit on midship bending moments in the Mariner-type ship being reached in regular waves of height significantly less than the theoretical upper limit of stability for progressive waves ( $h/\lambda = 1/7$ ). The experiments included variation of distribution of loading and of freeboard as model parameters. Each variation was tested at various speeds in regular head and following waves of several different lengths and of a wide range of heights. No significant upper limit of bending moment was found. However, the study establishes more firmly the grossly linear dependence of midship bending moment on wave height, even for extreme wave heights which may be encountered in service. These findings strengthened the case for determining design wave bending moments on the basis of statistical analyses of ocean waves and/or resulting bending moments.

# CONTENTS

	<u>Page</u>
Introduction . . . . .	1
Models . . . . .	2
Description of Apparatus . . . . .	6
Test Procedure . . . . .	11
Test Program	
A. Preliminary Tests . . . . .	12
B. Final Test Program . . . . .	14
Data Reduction . . . . .	14
Test Results . . . . .	
A. Compilation . . . . .	19
B. Condensation of Test Results . . . . .	20
Analyses	
A. Comparisons with Other Test Data . . . . .	34
B. Classification of Trends . . . . .	35
C. Maximum Bending Moments in Waves of Fixed Height . . . . .	37
D. Approximate Hydrodynamic Bending Moments . . . . .	40
Discussion	
A. Trends of Bending Moment with Wave Steepness . . . . .	42
B. Trends of Motions Amplitudes with Wave Steepness . . . . .	45
C. Results of Numerical Classification of Trends with Wave Steepness . . . . .	45
D. Additional Confirmation of the Results of Section C . . . . .	48
E. Maximum Moments in Waves of Constant Height . . . . .	48
F. Comparisons between Models . . . . .	48
Conclusions . . . . .	51
Recommendations . . . . .	51
Acknowledgements . . . . .	51
References . . . . .	51
Nomenclature . . . . .	52
Appendix . . . . .	54

NATIONAL ACADEMY OF SCIENCES-NATIONAL RESEARCH COUNCIL

Division of Engineering & Industrial Research

SR-157 Project Advisory Committee  
"Model in Extreme Waves"

for the

Ship Hull Research Committee

Chairman:

Mr. M. G. Forrest  
Gibbs & Cox, Inc.

Members:

Mr. Harold Acker  
Bethlehem Steel Co.

Mr. T. M. Buermann  
Gibbs & Cox, Inc.

Professor C. Ridgely-Nevitt  
Webb Institute of Naval Architecture

Professor W. J. Pierson, Jr.  
New York University

## INTRODUCTION

Knowledge for design purposes of extreme wave bending moments on ship hulls in irregular storm seas is restricted to a relatively limited number of full-scale ship observations. Theoretical methods presently available for predicting hull bending moments in regular waves are also limited to prediction in moderate wave heights in which the effects are considered to be roughly linear. Efforts are currently being made toward determining design wave bending moments on the basis of statistical analyses of full-scale and model data, an approach which requires considerable expenditure of time and funds.

A possible alternate approach was detailed in Ref. 1 (project 24) and a pilot study was made in the background work of that reference. This approach involved the possibility that an upper limit on midship bending moments might be found by the use of models in very steep tank waves. In the pilot study reported in Ref. 1, a model of a T-2 tanker was tested at zero and low speeds in head waves of model length and average heights ranging from  $L/20$  to  $L/8.5$ . The measured midship bending moment amplitudes, plotted against local wave height, showed considerable scatter in the higher waves. Nevertheless, two tentative conclusions were drawn:

1. There appeared to be a tendency for the bending moment to fall off from a linear relationship with wave steepness as wave steepness was increased.
2. The highest recorded bending moments in head seas in the highest wave were between 10 and 20% greater than the results of conventional static  $L/20$  calculation.

These conclusions suggested that reasonable maximum values of hull bending moments might be established experimentally by tests in very steep model tank waves. Project 24 of Ref. 1 entitled "Maximum Physically Possible Bending Loads," recommends such experiments and has as its objective: "To determine on a physical, rather than statistical, basis the upper limit of longitudinal seaway bending moments and shear forces expected on various ship types."

The present investigation stems from that recommendation and the basic philosophy was retained, which was to make a broad study of hull bending moments in regular waves of extreme steepness to see if the indications cited in the pilot study could be more generally applied. In this investigation an attempt was made to cover as many of the known major variables as possible. Since data scatter in steeper waves was to be expected it was felt that any parametric changes of the ship or of ship types should be as radical as possible so that differences would not be obscured.

The investigation was divided into two major parts. The first part was to consist of a study of one ship type and was to include investigations into the effects of variations in freeboard and weight distribution for that ship type. The second part of the project was to be a study of two additional different types of ship.

This report covers the first part of the investigation and deals with experiments conducted with models of the Mariner type ship. The second part of the investigation is reported in Ref. 2.

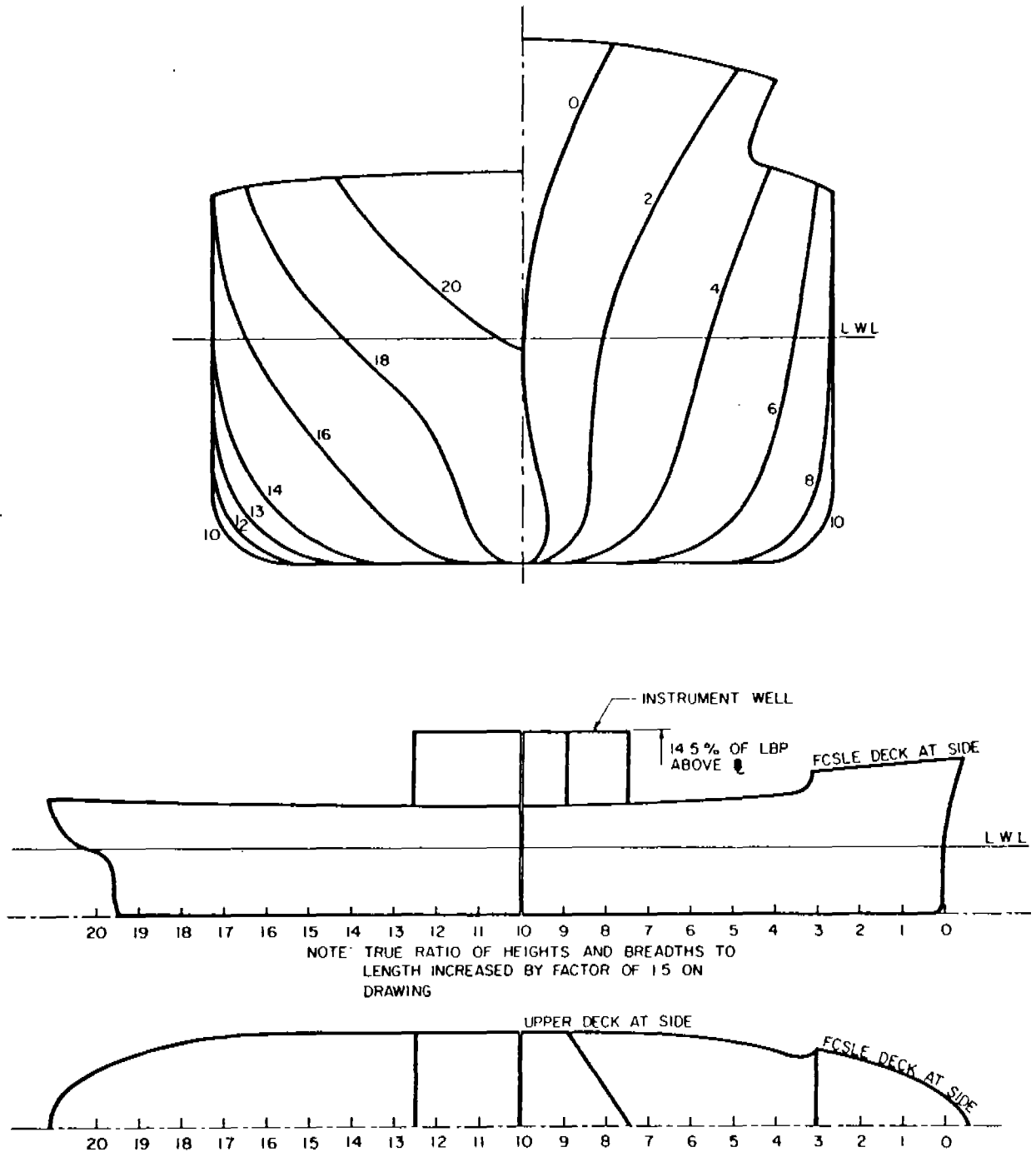


FIG. 1. MODEL DRAWING, BASIC MARINER HULL - MODELS 2251A-V1, 2251A-V2, 2251A-V3.

MODELS

It was decided to start the program with a dry-cargo ship type representative of good current practice in design and of a type likely to appear in quantity in the future. Under the present ship replacement building program, dry-cargo ships with speeds from 18 to 20 knots for merchant service and speed to 22 knots for naval

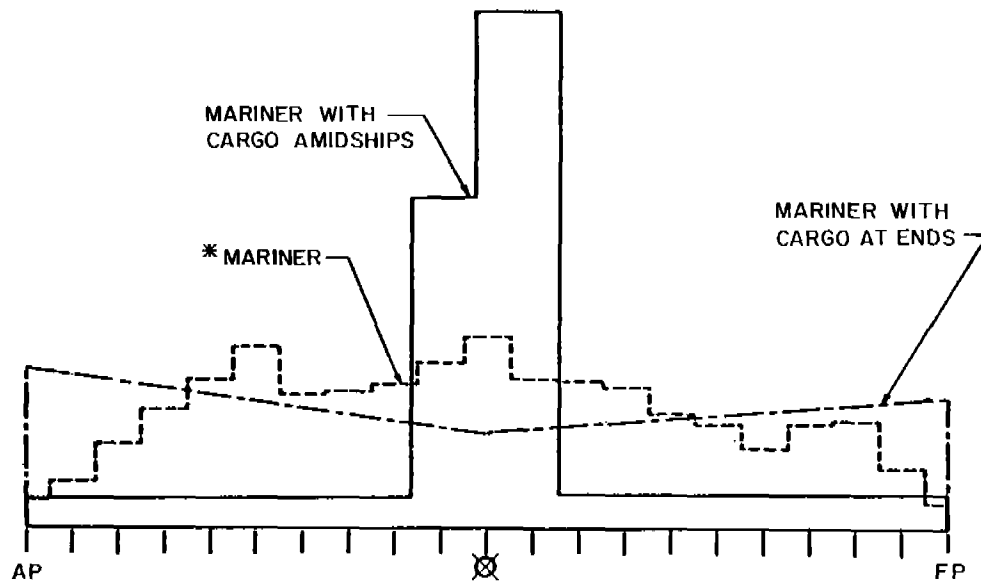
TABLE I. MODEL CHARACTERISTICS.

Model Number	2251A-V-1	2251A-V-2	2251A-V-3	2251E
Design	Mariner	Mariner	Mariner	Mariner with Increased Freeboard
Weight Distribution	Design	Cargo $\times$	Cargo-Ends	Design
Ship L.B.P., Feet	520.0	520.0	520.0	520.0
<u>MODEL CHARACTERISTICS</u>				
Nominal Model Scale	1:104	1:104	1:104	1:104
Length on 20 Stations, inches	60.00	60.00	60.00	60.00
Beam, inches	8.76	8.76	8.76	8.76
Prant, inches	3.20	3.20	3.20	3.22
Displacement, Pounds, F.W.	38.1	38.1	38.1	38.1
B/H	2.72	2.72	2.72	2.72
$C_b$	0.61	0.61	0.61	0.61
$C_M$	0.98	0.98	0.98	0.96
$\Delta/(L/100)^3$ , Design	140	140	140	140
LCB, % Station Length From $\times$	1.42 Aft	1.40 Aft	1.45 Aft	1.44 Aft
Scradius, % Station Length	24.3	15.9	30.3	24.2
Natural Pitching Period, Sec.	0.70	0.60	0.80	0.70
Natural Heaving Period, Sec.	0.75	0.75	0.80	0.75
Natural Frequency of Vibration, CFS	16.5	17.2	14.1	16.5
Freeboards: Aft, inches	2.30	2.30	2.30	5.48
Fwd, inches	4.05	4.05	4.05	5.48
V.L.L., inches	3.34	3.14	3.36	3.39
<u>HALF MODEL, FWD SECTION</u>				
Weight, lbs.	17.9	17.9	17.9	17.9
LCG Fwd $\times$ , inches	12.10	6.04	15.88	12.10
VCG, inches	3.32	3.46	3.43	3.34
$K_p$ , % Station Length/2	26.9	24.8	28.2	26.8
<u>HALF MODEL, AFT SECTION</u>				
Weight, lbs.	20.2	20.2	20.2	20.2
LCG Aft $\times$ , inches	12.32	6.93	15.72	12.33
VCG, inches	3.37	2.86	3.30	3.44
$K_p$ , % Station Length/2	25.5	21.8	32.0	25.5

transport service are common requirements. Most of the current designs of modern dry-cargo ships have coefficients and proportions generally similar to those of the Mariner type. Therefore, the original Mariner design was chosen as the basic hull design for the study. The parent Mariner hull model was designated as Model 2251A. Since there was to be a variation of weight distribution within the model, the designation V1 was added to the model number to denote the design weight distribution. Coefficients and characteristics of the parent Mariner model are given in the first column of Table I. A model drawing is shown in Fig. 1.

The model was made of wood, split in half at Station 10, and completely decked over except for an instrument well which was necessary to accommodate the towing apparatus and the bending moment balance amidship. Because of the anticipated amount of green water which would be on deck in tests in extreme waves, a deck erection which was expected to exclude the greater part of the water from the interior of the model was constructed in way of the instrument well, and extended upward to a level 14.5%L above the base line. The forward part of the raised well was made in the form of a breakwater to deflect the water rushing along the deck (Fig. 1). In preliminary testing it was found that an additional water deflector was necessary to keep spray out of the model and a "hat" was added to the forward part of the instrument well.

A suitable design weight distribution for this model was obtained from Ref. 3.



\* ALSO MARINER WITH INCREASED FREEBOARD

FIG. 2. WEIGHT DISTRIBUTIONS.

Since the technique for measuring bending moments was to be the jointed-model technique where two essentially rigid halves of the model are joined by a flexure beam, it was not necessary to reproduce the weight distribution exactly. The weight, longitudinal and vertical centers of gravity and the radius of gyration of each half of the model (as calculated from the weight distribution curve) were obtained in the model by adding suitable ballast after installation of weights simulating all apparatus. Values of weight, centers, and radius of gyration for each half of the model are given at the bottom of Table I.

The first variation on the Mariner design which was made was that of weight distribution. In line with the philosophy of making big changes it was determined to move as much ballast as possible in the Parent Mariner model, first toward amidship and then to the ends, keeping the total longitudinal center of gravity and the weight of each half of the model the same. After moving the ballast as far as possible in each direction and providing means of recapturing all three weight distributions at will, the resulting radii of gyration and centers of gravity of each half of the model in each of the two additional cases were measured. The characteristics of the two additional "models" produced by moving weights are given in Table I in the second and third columns. The variations were called Mariner, Cargo Amidships, Model 2251A-V2 and Mariner, Cargo at Ends, Model 2251A-V3. It may be noted from Table I that considerable change in radius of gyration of the entire model was achieved. From a normal figure of 24% of the length, it was possible to make sufficient change to achieve a gyradius of something less than 16% of the length for Model 2251A-V2, and to increase the gyradius to something in excess of 30% of the length for the 2251A-V3 model. These represent changes in gyradii

probably far beyond the range which is practically feasible. To aid in visualizing the amount of change involved, weight distributions for both the Mariner with Cargo Amidship and the Mariner with Cargo at Ends were derived from the centers and moments of inertia measured in the model. These two possible weight distributions are plotted in Fig. 2 and compared with the design weight distribution of the Mariner. In order to facilitate calculation, simple geometric forms were assumed.

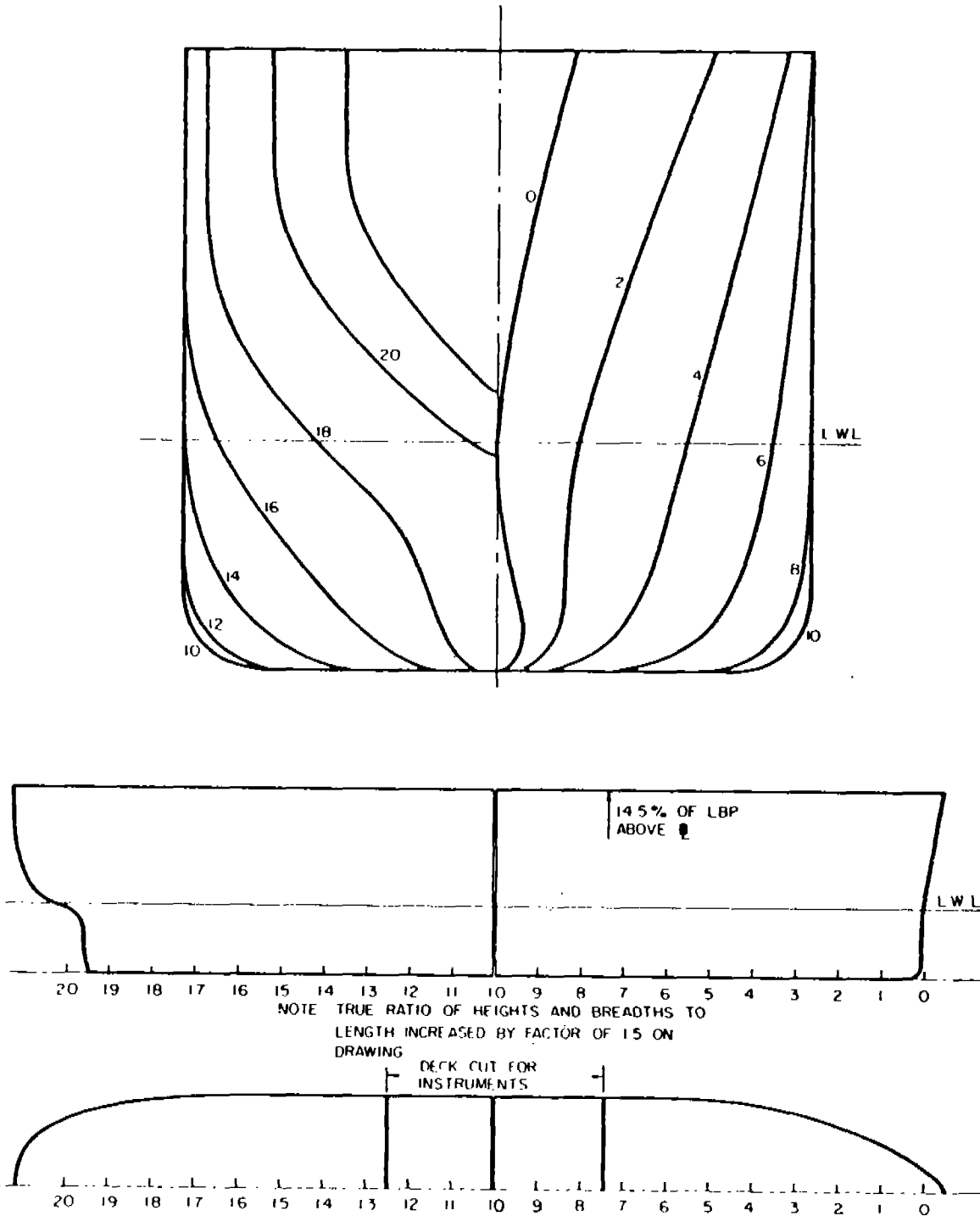


FIG. 3. MODEL DRAWING, MODEL 2251B - MARINER WITH INCREASED FREEBOARD.

The second major model parameter change was a variation in freeboard. Figure 3 shows a model drawing of the Mariner with Increased Freeboard, Model 2251B. The freeboard was increased to the same height as the top of the instrument well in the parent model. No sheer was given the model. It may be noted from Fig. 3 that such an increase in freeboard necessitated a change in the lines of the flare forward of Station 5. Had the original sections of the Mariner been extrapolated to the new

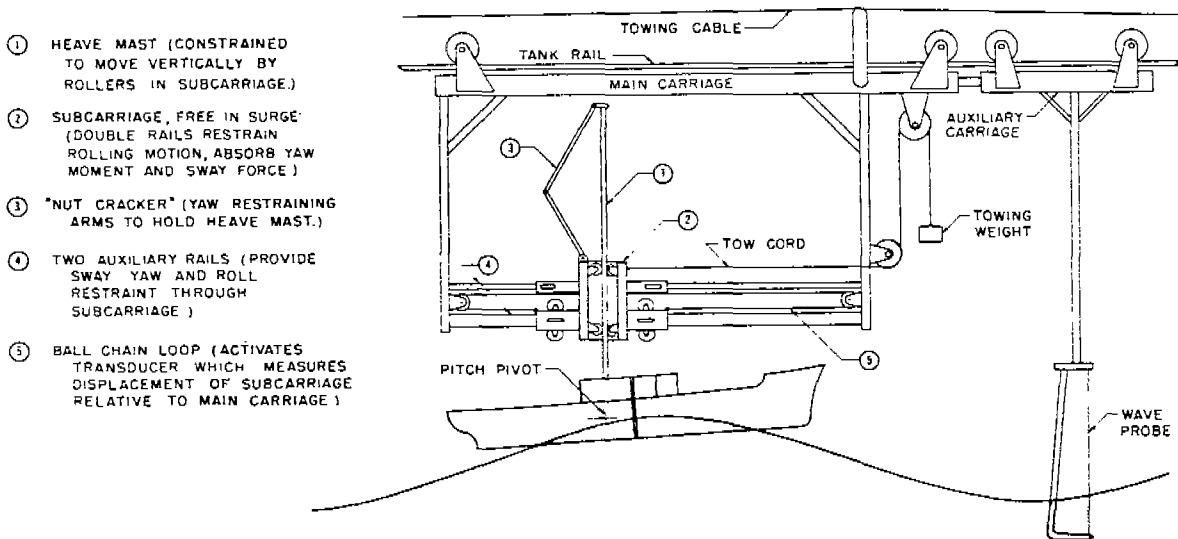


FIG. 4. SCHEMATIC OF TOWING APPARATUS.

freeboard, an unusual aircraft-carrier-like merchant ship design would have been the result, and it was felt that this was to be avoided. The model was decked over except for a space amidship as shown in the figure. No raised instrument well was built on this model as it was felt that there would be little water on deck. It was found during the tests that at times thin sheets of spray ran over the deck of the model and therefore a sheet-metal breakwater was added just forward of the instrument well. Coefficients and characteristics of this model are shown in the fourth column of Table I. It can be noted that the weights, centers and longitudinal gyradii are the same as that of the parent Mariner and thus the weight distribution of this model can be assumed to be the same.

After final ballasting, the natural pitching and heaving periods of all models were obtained by manual oscillation in a wide tank, in accordance with standard practice in Davidson Laboratory.

To summarize: the four models make up two studies. The first three shown in Table I make up a study of weight distribution, and the first and the fourth make up a study of the effect of freeboard.

#### DESCRIPTION OF APPARATUS

A schematic drawing of the mechanical test apparatus is given in Fig. 4. All models were attached to a towing apparatus which allowed freedom in pitching, heaving and surging motions, and restraint in yaw, sway and surge. The apparatus permitted the model to be oriented bow towards the waves or away from the waves in DL Tank No. 3 (300'x12'x6'). This apparatus consists of a main carriage with an auxiliary rail and a subcarriage to which is attached a vertical mast. The mast is restrained against all motions except vertical translation by ball bearing rollers. The subcarriage carrying the vertical mast is itself restrained against all motion except fore and aft translation. The model is attached to the bottom of the mast by pivots with axis athwartships thus allowing freedom in pitch and restraining rolling motion.

A gravity weight towing system was employed, Fig. 4, in which a falling weight provided a force between the main and the sub carriages. This force was transmitted through the pitch pivots to the model and caused the model and sub-carriage to move, resulting in a change in the relative distance between the

subcarriage and main carriage. This distance was measured and used as an error signal in a servo system which controlled the main carriage so as to minimize changes in relative position of main and sub carriages. If forward speed was required, a towing force was applied to the model from the falling weight system, the model then proceeded at whatever speed it would, and the main carriage followed. Tow forces could be applied in either direction. Since this method provided no means of accelerating the model, the model was accelerated by hand from the starting position. After the model reached the end of the run, the towing weight was electrically dropped out and the model then slowed down of its own accord. The recording run was about four model lengths for runs in which the model moved at speed. The elapsed time from one end of this run area to the other was measured in order to derive average model speed. In addition, in most of the runs, a continuous record of speed was obtained by a tachometer and roller fixed between the model subcarriage and the main tank rail.

Heaving and pitching motions were measured by potentiometers attached to the vertical mast and to the pivots in the model. Because of the heavy concentrated instrumentation loads in the models it was not possible to satisfy simultaneously the ballasting requirement and the requirement that the heaving motion be measured at the center of gravity. Therefore the pitch pivot and thus the measuring point for heave was located between six and eight inches aft of the LCG depending on the model, and an electronic circuit was devised to correct the resulting heave transducer signal from "heave at the pitch pivot" to "heave at the LCG." This correction was made in linear fashion in accordance with the following equation:

$$Z_{LCG} = Z_{pp} + a\theta, \text{ where } a = \text{distance from pitch pivot to LCG}$$

Two special wave probes were constructed for this project, each of an unusually large size to accommodate the unusually large waves envisioned. The wave probes were of the resistance type, two feet long, and designed for use in a plus or minus six inch range. Linearity of the probes was within one percent of the full scale range, that is: static calibrations of these wave wires showed results which nowhere deviated from a fitted straight line by more than one percent of the maximum range of the calibration. The wave probes were located approximately five feet ahead and five feet astern of amidships on the model, on the centerline of the tank for the tests of the first two models. Preliminary analyses of the results of these tests indicated that in following seas the distortion of the waves at the stern of the model by the model-generated waves was negligible, and the down-wave wave probe was omitted in subsequent testing.

A drawing of the bending moment instrumentation installed is shown in Fig. 5. A new bending moment balance system was designed for these experiments with a departure from previous practice; that is instead of attempting to achieve a frequency of model vibration equivalent to the scaled down frequency of vibration of the fundamental mode of the ship, the natural frequencies of the model plus balance system were kept as high as possible to provide a flatter frequency response at encounter frequencies. The balance consisted of an aluminum beam six inches long, 11/16 inch high and 1-1/16 inch wide connecting the two halves of the model (Fig. 5). In order to avoid hysteresis the beam and attachment flanges were machined out of the same piece of aluminum. The moment of inertia of the beam in vertical bending is  $2.88 \times 10^{-2} \text{ inch}^4$ . This value was selected as a compromise between the requirement of as high as possible natural model frequency and the requirement that measurable deflections result. The relative angular deflections at both ends of the beam were measured by differential transformer units. The two transformers were wired together in such a way so as to give a signal proportional to pure bending deflection of the beam. The mechanical design of the deflection pickups was such that an acceleration

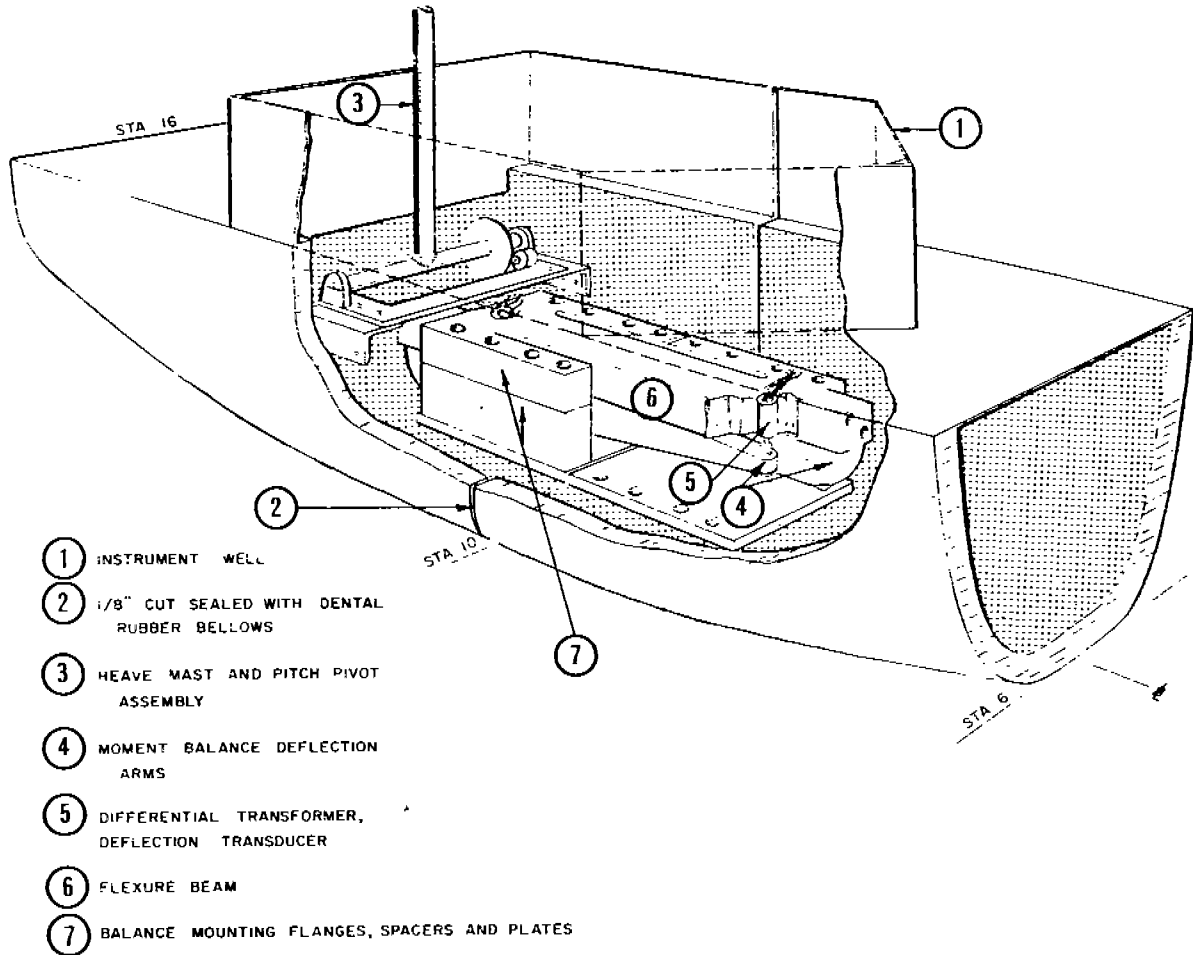


FIG. 5. ARRANGEMENT OF INSTRUMENTATION IN A TYPICAL MODEL.

of 1-g in a vertical direction would indicate a moment of less than one inch-pound. This error magnitude is approximately one percent of the highest moment measured. The acceleration standard is about twice the highest heave acceleration encountered and it is felt that no effects on the results due to vertical acceleration of the balance would be significant. Because of the design of the beam, the influence of shear between the two ends of the beam on the bending moment signal was extremely small. Coupling checks indicated 0.2 of an inch pound of bending moment for a 7 lb. pure shear between the two ends of the beam. Seven pounds of pure shear is considerably more than was expected in the test, and 0.2 in-lb. is a practically negligible error.

The same moment balance was used in all models. It was simply taken out of one model and put into the next, as required (Fig. 5). The joint between the two halves of each model was sealed by a thin rubber bellows. The natural frequencies of vibration of all four models are shown in Table I. Calibration of the balance was done with the model in the water by applying couples equal and opposite to the forward and after part of the model and recording the resulting signals. Linearity of the static calibration was within one percent of full scale, that is, within the reading tolerance of the oscillograph records. Previous experience with the jointed model technique indicated that the jointed model could be approximated by a single degree of freedom vibratory system and this assumption shall be used in the subsequent analysis with experimentally obtained natural frequencies and damping de-

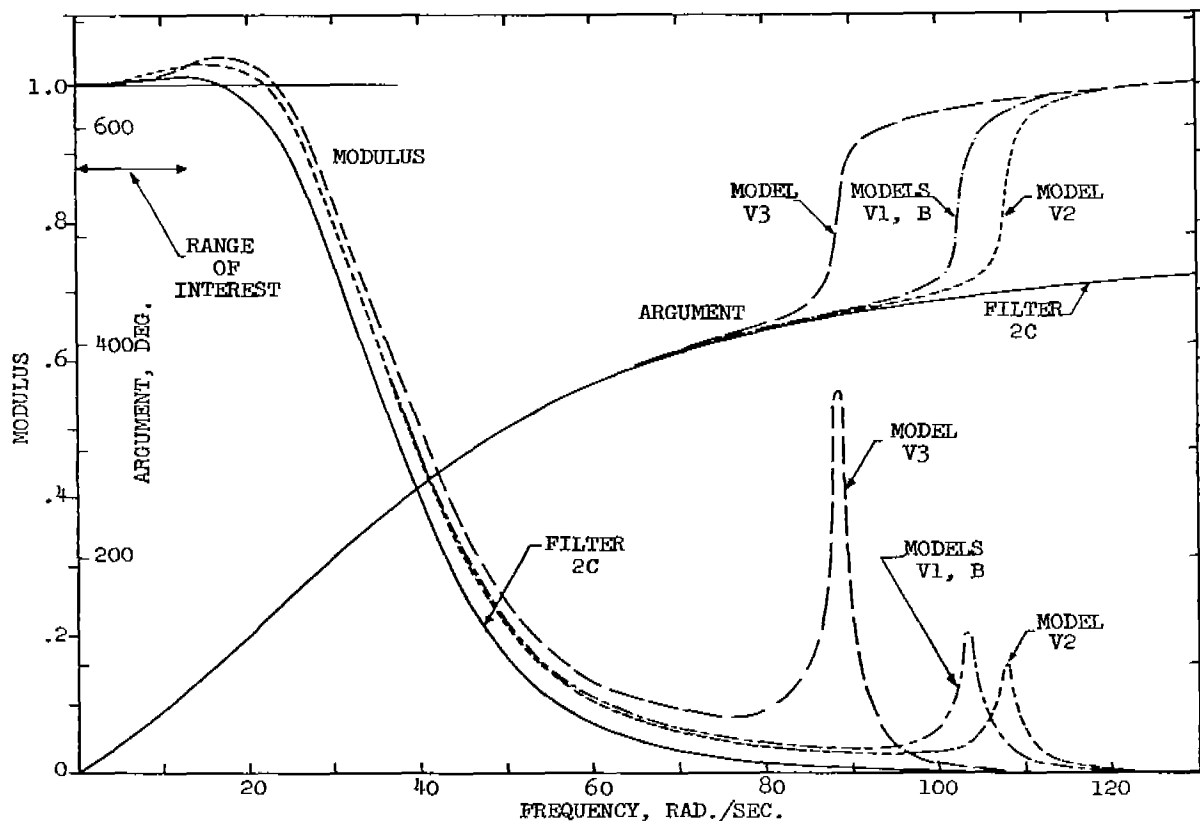


FIG. 6. FREQUENCY RESPONSE OF BENDING MOMENT MEASURING SYSTEMS.

fining the vibratory system.

To summarize, the instrumentation was arranged so that signals proportional to midship bending moment, pitching motion, heaving motion, wave elevation up-wave from the model (and down-wave, on occasion) and speed were available. These signals were recorded on a standard carrier amplifier-photographic oscillograph system.

Because previous experience had indicated that the bending moment record in extreme waves would have a high noise content, an electronic low-pass filter was interposed between the carrier-amplifier and the oscillograph in the bending moment channel. This filter had the effect of removing a good deal of the high-frequency vibration and making the bending moment record clean and easy to measure. It had the disadvantage of introducing a phase lag into the system and in complicating the transient response of the measuring system somewhat. Under the assumption that the signal from the bending moment balance and the real bending moment were related by the equations of a single degree of freedom elastic system, the effective frequency response of the bending moment measuring system was derived by combining the single degree of freedom elastic system corresponding to the measured model frequency and damping with the measured frequency response curve of the filter. Results are shown for all four models in Fig. 6. The frequency response represented is that of the response of the oscillograph to real bending moment. Both the amplitude and phase (modulus and argument) are shown. The maximum frequency range of interest shown in Fig. 6 is that dictated by the maximum head sea speed in the shortest wave length tested. Corrections for the frequency response of the measuring system within this frequency range were applied to the data but as can be seen were not highly significant. The resonance peaks of each model can be seen in Fig. 6 and the characteristic phase shift through  $90^{\circ}$  at resonance of a single degree of freedom elastic

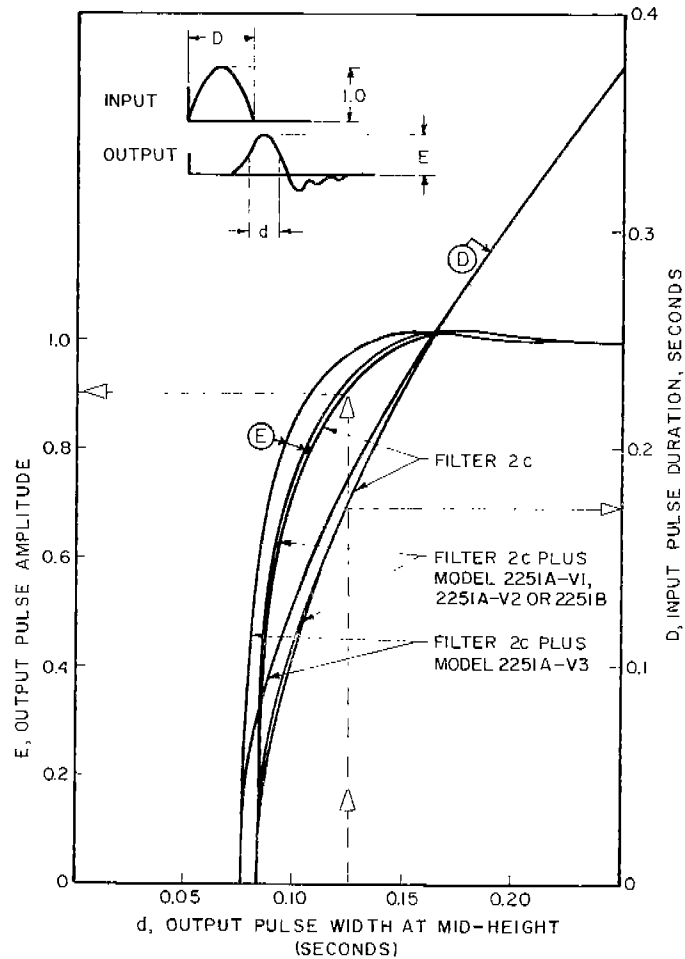


FIG. 7. TRANSIENT RESPONSE OF BENDING MOMENT MEASURING SYSTEM TO HALF-SINE PULSE.

system can be seen superimposed on the phase shift of the filter.

Because impacts were known to occur in tests of models in extreme waves, it was thought that a fairly crude transient analysis of the measuring system was in order. To do this, the frequency response functions shown in Fig. 6 were transformed on an IBM 1620 computer into impulsive response functions using a numerical complex Fourier transform program. These impulsive response functions allow the transient response to arbitrary inputs to be calculated using a convolution integral technique (Ref. 4, among others). It was felt that half sinusoid pulses might approximate pulses to be expected in the tests. Transient response to half sine pulses of various durations were calculated on the computer and the results of significance were abstracted into Fig. 7 in a form helpful to the analysis of oscillograph records. The small sketch at the top of Fig. 7 illustrates the nomenclature. The abscissa of Fig. 7 is the output pulse width at mid-height of the first excursion ( $d$ ). The term ( $E$ ) denotes the maximum value of the first excursion of the output under the influence of a half sinusoid input of unit amplitude. " $D$ " designates the input pulse duration. It can be seen from the curves of " $E$ " that the output pulse amplitude and the input pulse amplitude for all of the models covered in this report are perhaps within one or two percent of each other so long as the output pulse width ( $d$ ) is 0.15 sec. or greater. For output pulse widths at mid-height between 0.1 and 0.15 sec. errors of from 1 to 20% may be expected. For output pulse widths below a tenth of a second, large distortions are to be expected and, in fact, no output pulse widths below approximately 0.08 sec. are to be expected. Therefore if an input pulse from a severe slam is of very short duration, say less than a hundredth of a second, the output

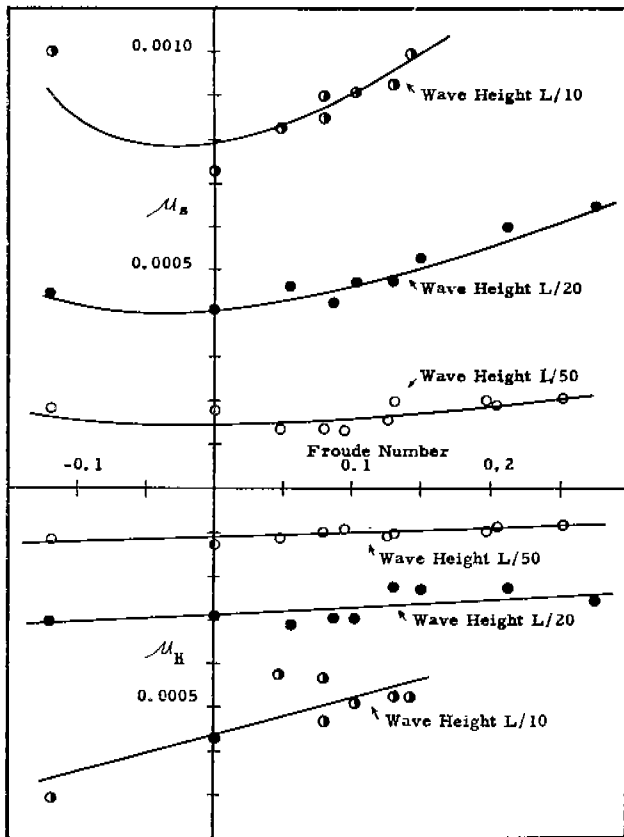


FIG. 8. MODEL 2251A-V1, MARINER: VARIATION OF BENDING MOMENT AMPLITUDES WITH SPEED IN HEAD 1.0L REGULAR WAVES.

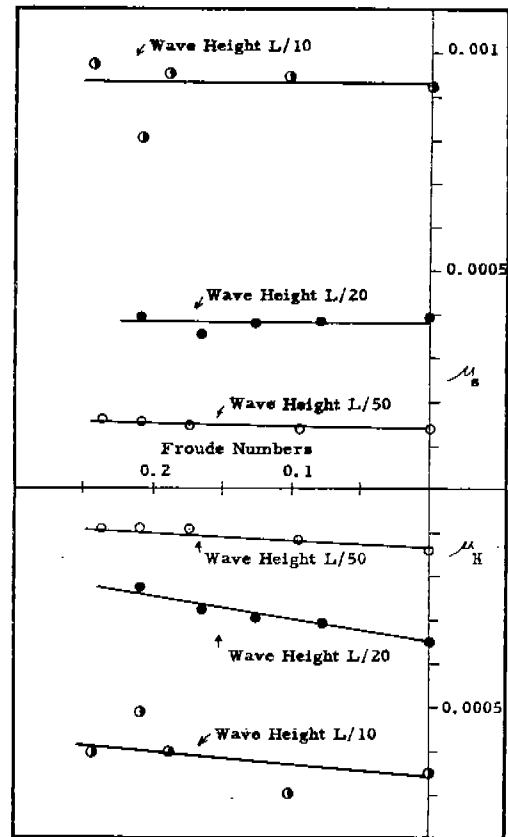


FIG. 9. MODEL 2251A-V1, MARINER: VARIATION OF BENDING MOMENT AMPLITUDES WITH SPEED IN FOLLOWING 1.0L REGULAR WAVES.

pulse for Model 2251A-V1 will be about 0.085 sec. but its magnitude will probably be less than one percent of the input magnitude. Unless very short duration pulses have extreme magnitudes, the measurement system will suppress them. Translated into ship terms, one would expect events occurring over a duration of time in excess of 1-1/4 sec. to be represented; events which occur over a duration time of less than one second to be suppressed.

#### TEST PROCEDURE

After calibrating each item to be measured, electrical check signals were put on about every third record taken to expose any electronic drifts in the system and closing calibrations were usually carried out at the end of the testing day. Static calibration results remained steady over a period of two or three test days. Calibration constant differences due to sensitivity drifts in the electronic apparatus seldom were more than 3% over such a period.

For each run the wavemaker was adjusted to give the desired period and stroke, the wavemaker was started and, in the case of a run at speed, the model was accelerated by hand when the test area (a 100 ft. length of DL Tank No. 3 adjacent to the wavemaker) was filled with waves. Because the towing apparatus was servo operated, the model attained a more or less constant speed and would proceed up (or down) the tank through the run area. The elapsed time it took the model to traverse the run

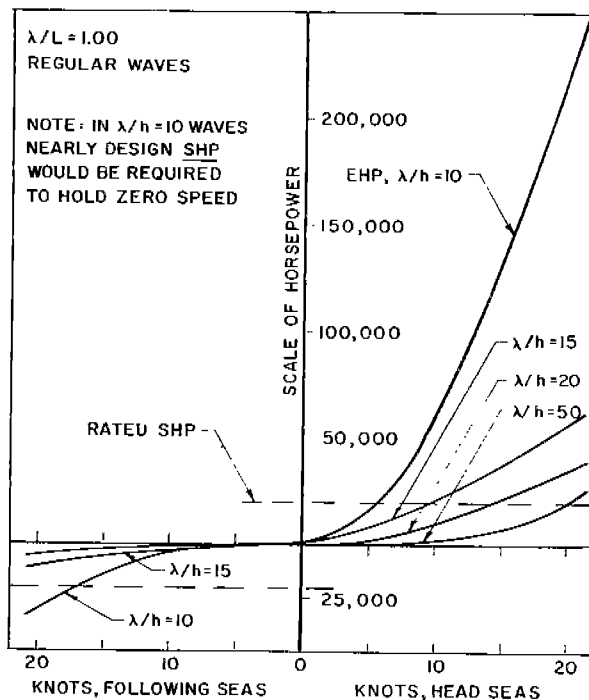


FIG. 10. EFFECTIVE HORSEPOWER IN REGULAR WAVES, MODEL 2251A-V1, PARENT MARINER.

area was recorded and an oscillograph record was made simultaneously of all the measurements while the model was in the run area. After the model proceeded out of the run area, the oscillograph record was shut off and the towing weights were dropped off to slow the model down and eventually stop it. For tests at zero speed it was found necessary to bypass the servo drive and to allow the towing weights and extremely weak springs to govern the relative motion between the model sub-carriage and the stationary main carriage. In this condition the model was located in the middle of the test area.

TEST PROGRAM

A. Preliminary Tests: While the effect of forward speed on bending moments in waves of moderate steepness is known to be small, it was not known initially whether the same tendency existed for extreme steep waves. It was therefore decided to do a preliminary test using the Parent Mariner model to determine the magnitude of the speed effect on midship bending moments in extreme waves. This preliminary test also served to shake the bugs out of the test procedure and the instrumentation. Results of the preliminary test for bending moments are shown in Figs. 8 and 9. These figures show the variation with speed of wave bending moment in model length waves of three nominal heights. The bending moments are separated into hogging and sagging moments ( $\mu_H$  and  $\mu_S$ , respectively, see Data Reduction). Speed is given in terms of Froude number.

Figure 8 shows the bending moment amplitudes in 1.0L regular head waves. It can be seen from this figure that the general trends of bending moments in very steep waves are not too different from those in moderate waves. The data for the L/10 waves ends at a Froude number of about 0.15. It was felt impossible to run the Mariner model, without swamping, at higher Froude numbers in this wave steepness although speeds in excess of this could be obtained in the lower wave heights. Figure 9 shows trends of bending moment in following regular waves at speeds of from zero to a Froude number of approximately 0.23. This figure also shows that changes in bending moment with speed are relatively small and indicates that data need not be obtained at fine speed intervals.

TABLE II. TEST PROGRAM MARINER MODEL AND VARIATIONS.

Model 2251A-V2		Hull as Designed "Cargo" Moved Amidships					
Heading	Speed Classif.	Wave Length/Model Length					
		.50	.75	1.00	1.25	1.50	1.75
180°	Zero		5*	5*	5*	5*	4*
"	Forward		4	5	5*	5	4
"	Drifting		6	6	5*	5	4
0°	Zero			5	5	5	
"	Forward		5	5	5	6	4

Model 2251A-V1		Hull as Designed Design Weight Distribution						Model 2251B		Radical Increase in Freeboard Design Weight Distribution					
Heading	Speed Classif.	Wave Length/Model Length						Heading	Speed Classif.	Wave Length/Model Length					
		.50	.75	1.00	1.25	1.50	1.75			.50	.75	1.00	1.25	1.50	1.75
180°	Zero	4	6*	7*	8*	8*	5*	180°	Zero		4*	5*	5*	5*	4*
"	Forward		4	6	5*	5	6	"	Forward		4	5	5*	5	4
"	Drifting		4	5	5*	5	4	"	Drifting		4	5	5*	6	4
0°	Zero	4	6	6	8	7		0°	Zero			5	5	5	
"	Forward		4	7	5	5	4	"	Forward			3	5	5	

Model 2251A-V3		Hull as Designed "Cargo" Moved to Ends					
Heading	Speed Classif.	Wave Length/Model Length					
		.50	.75	1.00	1.25	1.50	1.75
180°	Zero		4*	5*	6*	5*	4*
"	Forward		4	5	5*	5	4
"	Drifting		4	5	5*	5	4
0°	Zero			5		5	
"	Forward			5		5	

a. Numbers in the blocks indicate the number of good runs obtained in order to cover the range of wave heights. Blanks indicate no runs attempted.

b. \* Indicates a motion picture record of the model in the highest wave.

Figure 10 shows an estimated effective horsepower derived from the tow forces used in the preliminary test in 1.0L regular waves. It is shown that as far as the head seas case is concerned, the effective horsepower requirements in extremely steep waves at speeds above 5 knots are considerably more than the rated shaft horsepower of the ship. It is doubtful if the designed shaft horsepower would allow the ship to maintain headway.

Two conclusions drawn from this preliminary test were (1) that it was impractical and possibly unnecessary to attempt to obtain data at forward speeds in excess of a Froude number of 0.12 or 0.14, and (2) that as far as the head sea case was concerned, limitation of speed to three cases would be adequate for subsequent work. It was seen from Fig. 9 that an adequate definition in following seas could be obtained by taking zero speed and a forward speed near design speed. Furthermore, it was felt that such a speed simplification was vital to the project since it would vastly reduce the number of runs necessary.

A result from the preliminary testing which is not shown in these figures was obtained from tests of the parent Mariner model at zero speed in waves of from 1/2

the model length to 1-1/2 model length. Bending moments were surprisingly high in the very steep 1.50L waves. The moments were very low in the 0.5L wave length. This indicated that instead of testing over a range of wave lengths from 0.5 to 1.5L, as had been original planned, it might be better to concentrate on a wave length range between 0.75 and 1.75L.

B. Final Test Program: The final test program is detailed in Table II. The arrangement of the major blocks in Table II is suggestive of the model parameter variations involved. The blocks arranged vertically comprise the weight distribution investigation, the blocks oriented horizontally comprise the freeboard investigation.

Within each block is shown a table of variables. The standard test program resulting from the preliminary test results included five speeds, three speeds in head seas and two speeds in following seas. Zero speed runs were made in both head and following seas. A forward speed case in head seas was specified and in this case Froude numbers were held to about 0.13 plus or minus 0.01. The third speed case in head seas was the drifting speed. This speed was established for each wave length by allowing the model to drift astern at the speed produced by the highest wave generated. For waves of lower height and of same wave length the same astern speed was maintained by putting reverse thrust on the model. The forward speed in following seas corresponded to approximately twice the drifting speed attained in head seas. Because of the results in Figs. 8 and 9, it was felt unnecessary to reproduce exact model speeds for comparison of data obtained in different wave heights in the same wave length. Although six different wave lengths are shown in each block of Table II, only a few selected runs were taken in 0.5L waves. As is noted on the table, the numbers in the blocks indicate the number of runs which were obtained in order to cover the possible range of wave heights for each wave length at each speed. Since the forward speed case in following seas was extremely difficult to run, this case was de-emphasized in order to save on test time in the cases of models 2251A-V3 and 2251B. In general, more runs were attempted to cover the range of wave heights in the wave lengths of from 1.0 to 1.50L than were attempted in 0.75 and 1.75L waves. This decision was made purely from reasons of economy since roughly 400 good runs were required to meet the test program for the four models, and it was necessary to make about 600 runs in order to produce 400 good runs. This came about largely because it was not always possible to guess the correct towing weight to produce the proper model speed.

A standard motion picture taking routine was established at the end of the data-taking runs for each model. Motion pictures of model behavior were taken in waves of from 0.75 to 1.75L at zero speed and at the drifting and forward speed in head seas for a wave length of 1.25L.

#### DATA REDUCTION

It was decided to assess the magnitudes of moments and motions in waves by measuring the maximum and minimum of each cycle of the time histories obtained. For the waves and the pitch and heave motions, the sums of the maxima and minima were measured and tabulated (double amplitudes). For the bending moments, the maxima and minima (sag and hog) of the filtered bending moment trace were measured. This was done for as many cycles as possible up to a maximum total of 20. In the zero speed cases, between 16 and 25 cycles were recorded and up to 20 were measured and tabulated. Because of the instability of the waves and the variation in height from cycle to cycle, the average of the maxima, minima, and double amplitudes were calculated as were the root mean square deviations of these measurements from their respective means. The averages were used thereafter as test points. Most of the data handling after the initial measuring of the oscillograph traces was done on an IBM 1620 Computer.

All data were non-dimensionalized as much as possible in the course of the data reduction. Wave steepness was expressed as wave height to length ratio,  $h/\lambda$ , wave length was expressed as the wave length to ship length ratio,  $\lambda/L$ . The symbol  $2\theta$  stands for the double amplitude of pitch in degrees. The heaving double amplitude was divided by the model length to present heave results ( $2Z_o/L$ ).

All bending moment amplitudes were converted to a non-dimensional coefficient form. The form selected was the bending moment (hog or sag) divided by the quantity  $\rho g L^3 B$  where  $\rho g$  is the weight density of water,  $L$  is the model length,  $B$  is the maximum model beam. The coefficient normally used to express results from tests in moderate waves is similar but contains the wave height in the denominator. The two coefficients are related as follows:

If  $\mu$  = moment coefficient used herein

and  $C$  = moment coefficient used in moderate wave tests

$M$  = bending moment

$$\mu = \frac{M}{\rho g L^3 B}, \quad C = \frac{M}{\rho g L^2 B h}$$

$$\text{Then } \mu = C \cdot (h/\lambda) \cdot (\lambda/L)$$

Preliminary data reduction and presentation indicated that presentation of individual test points on charts where more than one wave length was included were confusing. It was felt that final conclusions would depend heavily on the lines faired through the test data, and that interpretation would depend to a great extent on the adequacy of fairing of mean lines through the test spots. Since some degree of subjectivity in fairing data was inevitable, it was decided to concentrate the subjectivity into the form of an equation to be fitted impartially to each set of data by the IBM 1620 Computer. The data was sorted into test groups each of which contained the data for all the various wave steepnesses obtained for a particular model, speed, heading and wave length. A curve was fitted to each of the resulting plots of average sagging moment, hogging moment and pitching and heaving amplitude vs. wave steepness. The form of the equation was as follows:

$$Y = a(h/\lambda) + b(h/\lambda)^N$$

Where:  $Y$  = bending moment, pitch or heave amplitude

$h/\lambda$  = wave steepness

$a, b$  = coefficients

$N = 2, 3 \text{ or } 4$

The computer actually fitted three such equations, one for each value of  $N$ , for each response and chose the best fit on the basis of the least residual mean square deviation from the test data. It then evaluated the resulting equation for values of  $h/\lambda$  convenient in plotting. The resulting fitted lines were judged to be of the form which would have resulted from hand fairing. No great significance is attached to the values of the coefficients obtained. The procedure followed was merely to insure consistency of method rather than to provide material for generalization. A two-term equation was selected to avoid over-fitting the test spots, on the basis of preliminary fitting with three and four term equations.

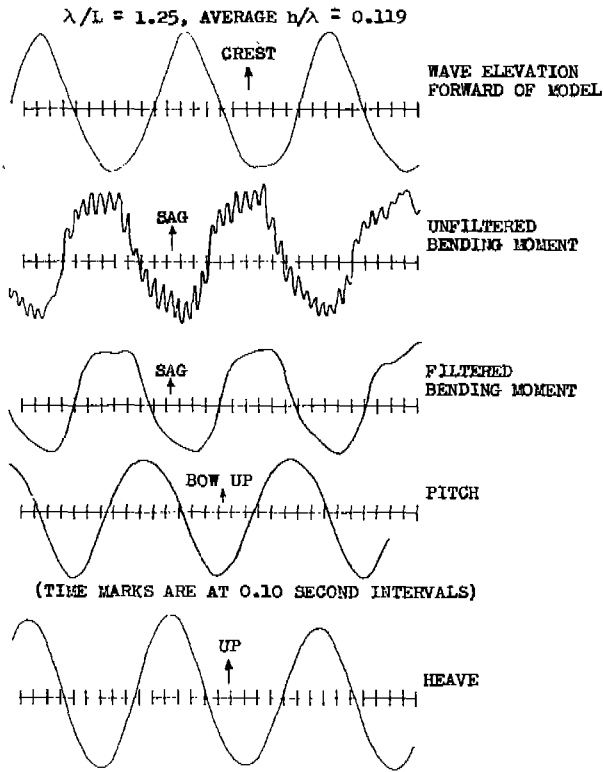


FIG. 11. SAMPLE OSCILLOGRAPH RECORD TRACING: RUN 216, MODEL 2251A-V1, PARENT MARINER, HEAD SEAS, ZERO SPEED.

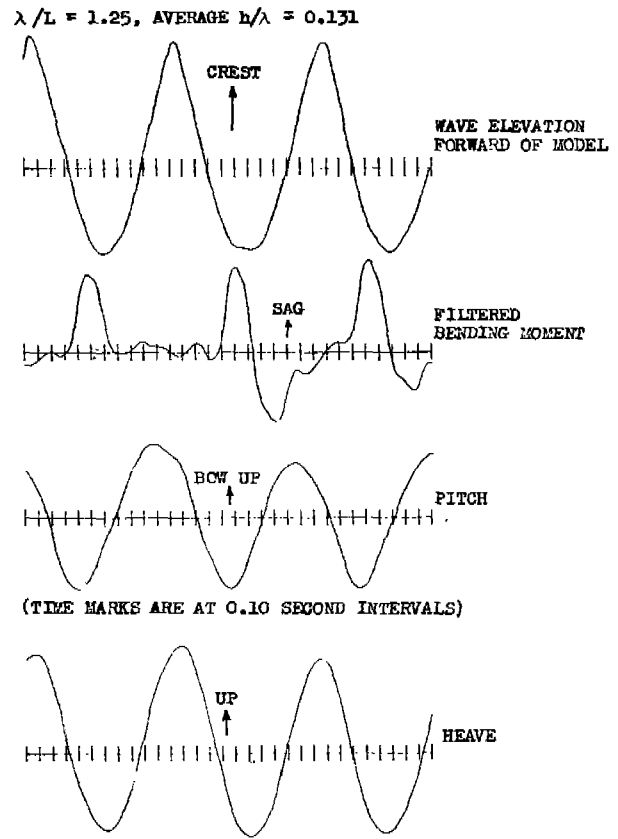


FIG. 12. SAMPLE OSCILLOGRAPH RECORD TRACING: RUN 880, MODEL 2251A-V1, MARINER, CARGO AT ENDS, HEAD SEAS, ZERO SPEED.

Since the emphasis in the analysis was to be on the bending moment amplitudes and the motions results were to be a by-product, no careful phase estimation was done. A crude phase estimate of the bow-up pitch motion lagging the sagging bending moment and of the up-heave motion lagging the sagging bending moment was made in each run. Since these phase measurements were quite crude and since they were of the same magnitude for all of the models and wave heights, at the same wave length and speed, an average value over all the models and wave heights was recorded for each wave length and speed.

Figures 11 and 12 show tracings of short sections of oscillograph records from two runs. Both runs are zero speed-head sea cases, the first for the Parent Mariner, and the second for the Mariner with Cargo at Ends. It may be observed from the two oscillograph records that there is apparently considerable difference in bending moment behavior between the Parent Mariner model and the Mariner with Cargo at Ends.

It may be of interest in Fig. 12 to observe the shape of the filtered bending moment trace. This was a reasonably common appearance of traces resulting from the steep wave experiments for this particular model. This model had frequent forward bottom impacts and the large sagging excursion in Fig. 12 occurs at about, or just after, the time that large forward bottom impacts occur. While these bottom impacts were audible, during the tests, the very sharp spikes of moment which they might

TABLE III. SAMPLE TEST RESULT TABULATION.

Model: <u>2251A-V1</u> - <u>Mariner, Parent</u>			Test Group: <u>1.1122125</u>										
Zero Wave Bending Moment Corresponds to a Still Water Moment of: <u>0.00047 HOG</u> 1.0L Static Calculations (Non-Dimensional)			Wave Length: <u>1.25L</u>										
			Heading: <u>180</u> Degrees										
<table border="1"> <tr> <td><u>Wave Height</u></td> <td><u>Wave Sag</u></td> <td><u>Wave Hog</u></td> </tr> <tr> <td><u>L/20</u></td> <td><u>0.00078</u></td> <td><u>0.00059</u></td> </tr> <tr> <td><u>L/10</u></td> <td><u>0.00154</u></td> <td><u>0.00114</u></td> </tr> </table>			<u>Wave Height</u>	<u>Wave Sag</u>	<u>Wave Hog</u>	<u>L/20</u>	<u>0.00078</u>	<u>0.00059</u>	<u>L/10</u>	<u>0.00154</u>	<u>0.00114</u>	Speed: <u>0.12 to 0.14</u>	
			<u>Wave Height</u>	<u>Wave Sag</u>	<u>Wave Hog</u>								
<u>L/20</u>	<u>0.00078</u>	<u>0.00059</u>											
<u>L/10</u>	<u>0.00154</u>	<u>0.00114</u>											
			Heave Tuning Factor: <u>0.90</u>										
			Pitch Tuning Factor: <u>0.85</u>										
Bow-up-Pitch Lags Sagging Moment Approx.:			<u>125</u>	Degrees									
Up-Heave Lags Sagging Moment Approx.:			<u>205</u>	Degrees									
Coefficients of Equation Fitted to Run Averages of Amplitude													
Y =	$M_s$	$M_H$	$Z_0$	$2Z_0/L$									
N	3	2	2	4									
a	.0110	.00641	440.	.876									
b	-.144	-.0128	-1897.	-17.9									
RMS Deviations of Measured Amplitudes within Each Run (Units consistent with those on plot)													
Run No.	248	255	257	219	218								
h/λ	.0493	.0690	.0865	.104	.118								
No. Cycles	20	20	20	14	15								
rms Wave x 10 <sup>2</sup>	.28	.43	.37	.63	.51								
rms Sag x 10 <sup>4</sup>	.31	.16	.21	.32	.68								
rms Hog x 10 <sup>4</sup>	.23	.12	.25	.31	.79								
rms Pitch, deg.	.73	.57	.55	.80	1.20								
rms Heave x 10 <sup>2</sup>	.46	.28	.26	.53	.40								
REMARKS: (1) Form of Equation: $Y = a(h/\lambda) + b(h/\lambda)^N$													
(2) Sagging moments in waves above $h/\lambda = .07$ increased by forward bottom impacts. Pulse duration believed long enough for amplitude resolution within 10 percent.													

produce has apparently not been picked up on the filtered moment trace. This was what would be expected from the transient response characteristics, Fig. 7. The excursions which remain have pulse widths at midheight of approximately 0.15 sec. and this, according to Fig. 7, means that the value of the maximum observed on the oscillograph record should be a good indication of the actual maximum wave bending moment experienced. In some of the records, mostly at the higher speeds, evidence was seen of some shorter duration pulses superimposed on the longer duration quasi-static moment. Since some of these pulses were the maximum of the record, some errors are introduced into the amplitudes in this manner. However, all reasonable views of each case, taking into account the data in Fig. 7, indicated that the

MODEL 2251A-V1 TEST GROUP 1.1122125  
WAVE LENGTH: 1.25 L MODEL HEADING: 180°  
APPROX MODEL SPEED  $v/\sqrt{gL} =$  0.12 to 0.14

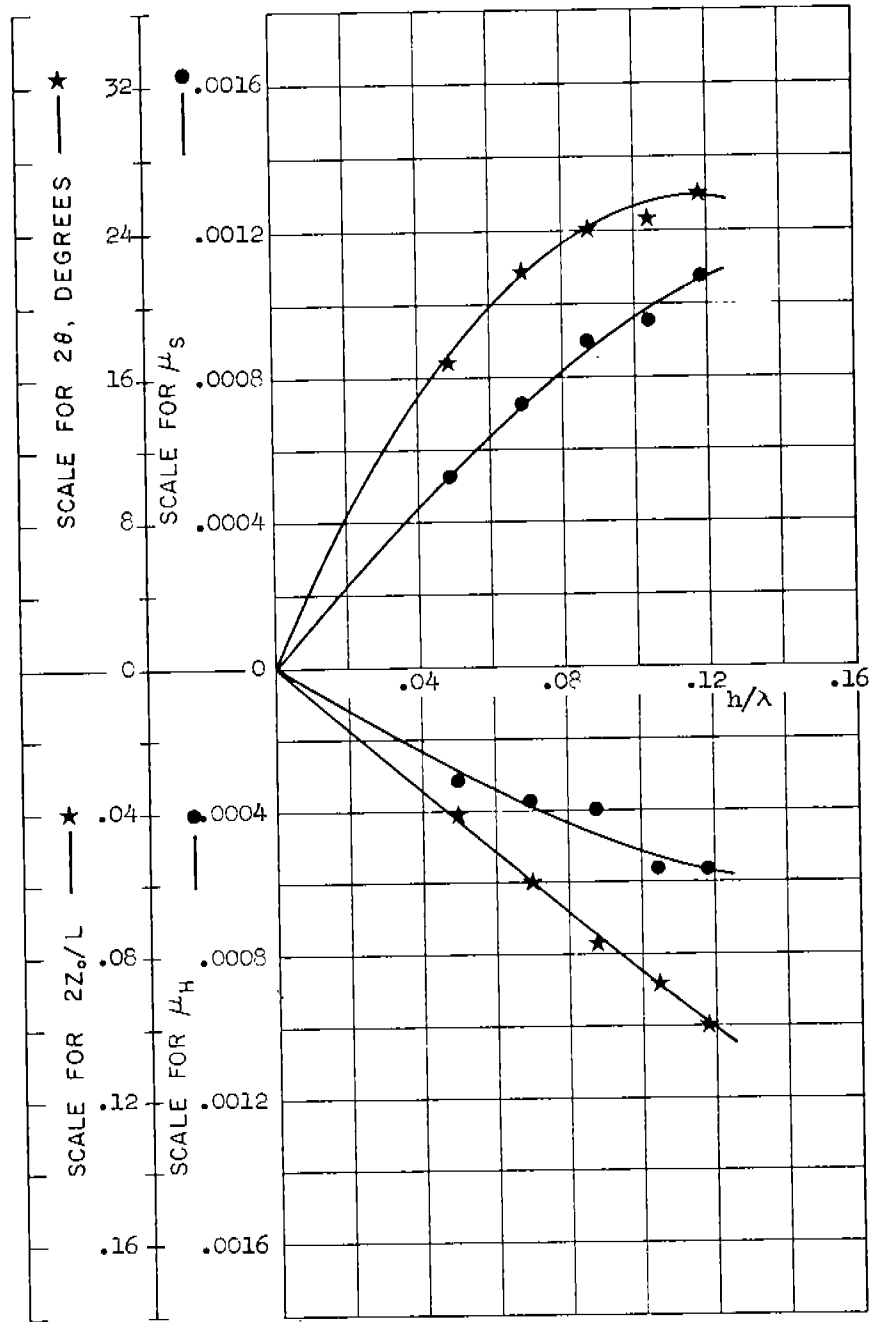


FIG. 13. SAMPLE BASIC DATA CHART.

under-estimate of bending amplitude which resulted from these superimposed pulses was not very great.

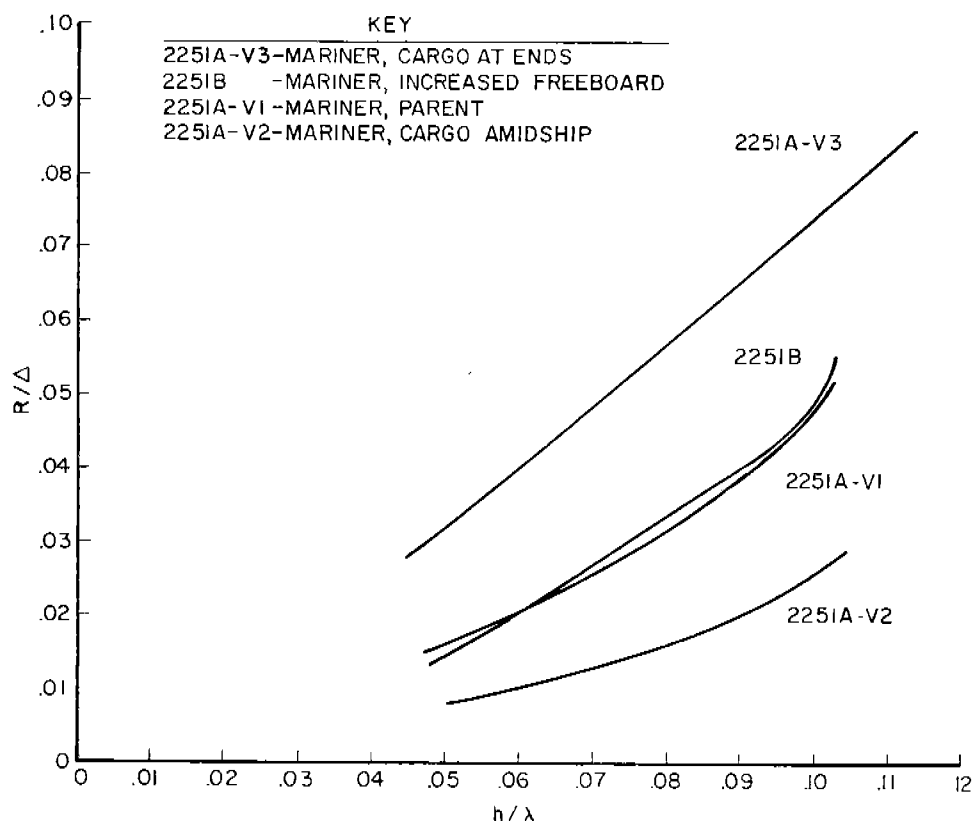


FIG. 14. UPPER ENVELOPE OF MODEL RESISTANCE IN WAVES OF ALL LENGTHS, HEAD SEAS, FR. NO. = 0.12 to 0.14.

TEST RESULTS

A. Compilation

Test results were grouped in accordance with the blocks in the test program of Table II, that is, all the data obtained in the same wave length, heading, speed and for the same model were grouped together. All basic test data are contained in Ref. 5, and because all the data consumes 168 pages of that reference, only a sample is presented herein. The data for each test group was summarized in two pages, one of which is a chart and the other a tabulation. Table III is a sample data tabulation, Fig. 13 the corresponding sample chart.

The chart, Fig. 13, shows the test spots and the fitted lines for the bending moment and motion amplitudes. Test spots for moments are shown as circles, those for motions as stars. All amplitudes are plotted to a base of wave steepness. The variability of the wave height measurement in the most severe wave was made the criterion by which the fitted curves were said to represent the test range of  $h/\lambda$ . The lines fitted to the amplitude data were extended in each case to a wave steepness corresponding to the average wave steepness observed in the most severe wave plus one and a half times the root mean square deviation of the wave height measurements in that run.

The supporting tabulation (Table III) in addition to indicating the model number, description, wave length, heading and speed, shows the heave and pitch tuning factors which are the ratios of the frequency of encounter to the natural

frequencies of oscillation. The tabulations also show the results of standard static calculations. These results are separated into still water moments and wave moments. The still water bending moments were obtained by calculations based on the hydrostatic properties of the model and the model ballasting results. The standard static wave moment calculations shown do not include Smith effect. Static calculations have been carried out for the Mariner at heights other than  $L/20$  ( $L/10$  and  $L/7$ ). Results for a static wave height of  $L/10$  are shown in the applicable tabulations. The values obtained in the static calculations for wave height of  $L/7$  were: (non-dimensionalized) wave sagging moment, 0.00169; wave hogging moment, 0.00146. Since the wave bending moment depends only on geometry of the model, the calculations are therefore valid for all of the three weight distribution variations. Since little hull lines change was made between Model 2251A and 2251B, the model with increased freeboard, the  $L/20$  static calculations are very likely approximately correct for model 2251B.

The tabulations (Table III) also give the approximate motion phase lags. Coefficients of the equations fitted to the average amplitudes measured are given. There follows a tabulation of the run number, the approximate average wave steepness measured, the number of cycles analyzed and the root mean square deviations of the measurements within each run. Where applicable, remarks are made in the tabulations pertaining to the existence of bottom impacts. These represent opinions formed during a check of the tape records against the applicable transient response curves of Fig. 7.

An analysis was made of the forces necessary to tow the models in head seas at the forward speed Froude number of 0.13. The upper envelope of all results are shown for each model in Fig. 14 where tow force per unit model displacement is plotted on a base of wave steepness. Differences in magnitude between tow forces in head and following seas for all models are well represented by Fig. 10.

Because of the bulk of the data to be analyzed and interpreted, it was felt of interest to attempt to simplify the process wherever possible. To this end the question was raised as to whether the data obtained in the following seas at zero speed and the data obtained in head seas at zero speed were near enough the same to make it possible to eliminate the interpretation and further analysis of all the following seas, zero speed results. The results presented in Fig. 8 and 9 indicated that this might not be an impossibility and therefore some detailed comparisons of bending results from zero speed tests in head and following waves of the Mariner parent, Model 2251A-V1, and the Mariner with Cargo Amidship, Model 2251A-V2, were made. Figures 15 and 16 show a comparison of bending moment results from zero speed tests in head and following waves for the Parent Mariner. Comparisons are shown for four wave lengths, all the average test spots are shown, as are the fitted curves. Figures 17 and 18 show the same comparison for Model 2251A-V2 in wave lengths  $1.0L$  and  $1.25L$ . It was felt that the agreement shown in these figures was sufficient to justify deferring the further analysis of the zero speed following sea case. While the trends of the fitted curves are somewhat different, the magnitudes of the test spots are very similar and in some cases almost identical. If a region of scatter were constructed about each data point, using  $1-1/2$  the tabulated rms deviations, most of these regions would overlap and thus indicate that differences measured in extreme waves between the head and following sea cases were (1) not great, and (2) perhaps not really significant relative to the accuracy of the experiment. No further analysis of the zero speed, following sea case was made.

### B. Condensation of Test Results

#### 1. Trends of bending moment with wave steepness.

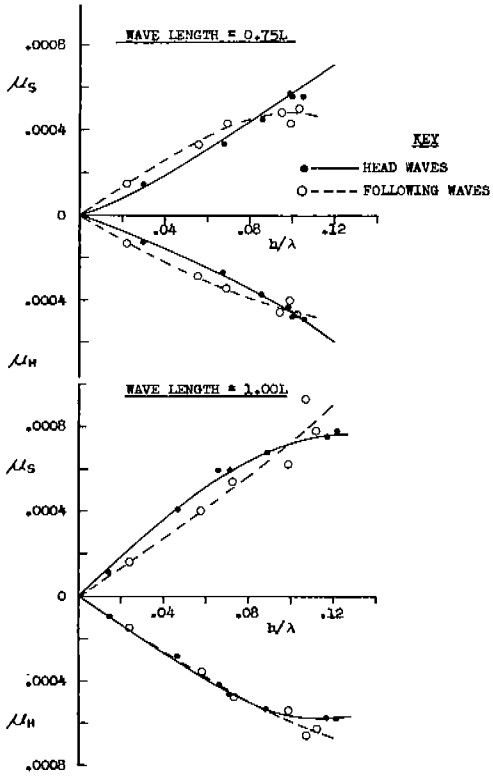


FIG. 15. MODEL 2251A-V1, PARENT MARINER.

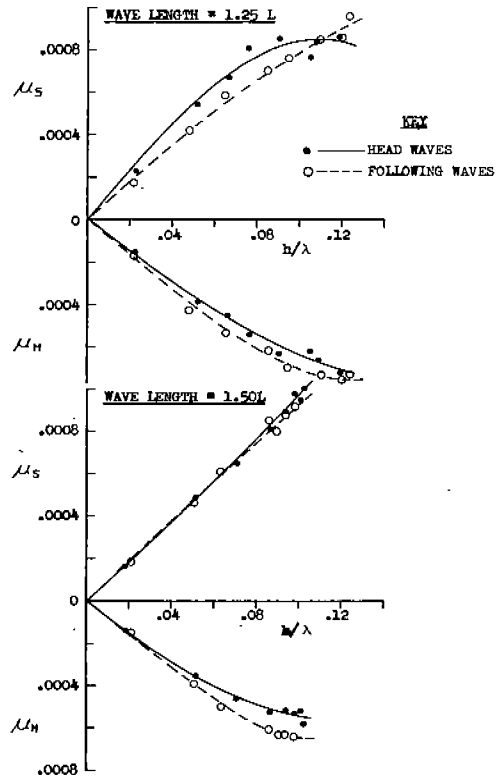


FIG. 16. MODEL 2251A-V1, PARENT MARINER.

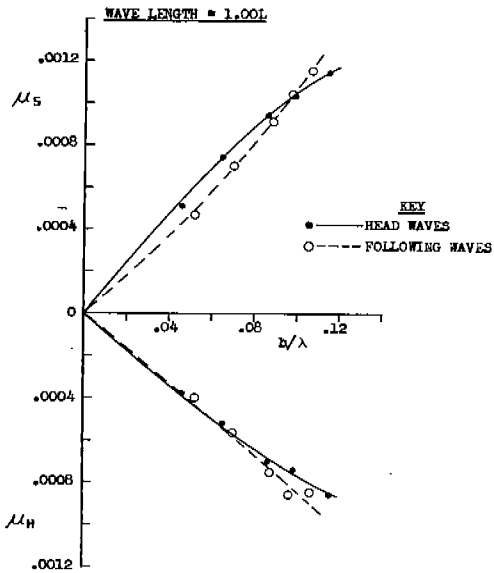


FIG. 17. MODEL 2251A-V2, CARGO AMIDSHIP.

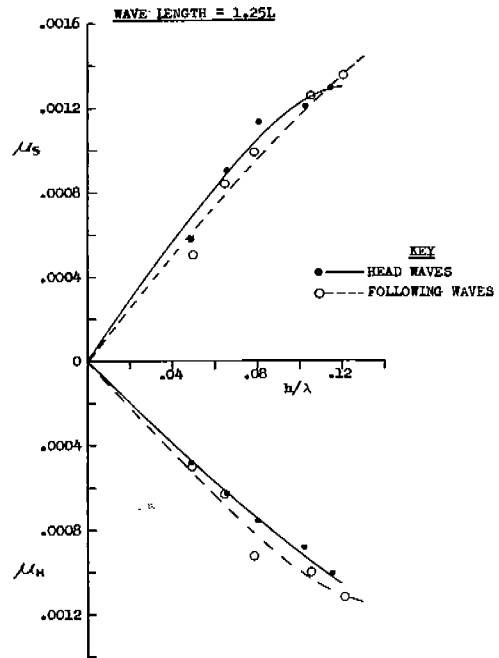


FIG. 18. MODEL 2251A-V2, CARGO AMIDSHIP.

FIG. 15-18. COMPARISON OF BENDING MOMENTS FROM ZERO SPEED TESTS IN HEAD AND FOLLOWING WAVES.

To simplify correlation and comparison the faired lines through time data applicable to each model (Ref. 5) in each speed-heading condition have been plotted together in Figs. 19 through 34. These figures are arranged in the following order:

- 19 - 22 Four models, head seas, forward speed
- 23 - 26 Four models, head seas, zero speed
- 27 - 30 Four models, head seas, drifting astern
- 31 - 34 Four models, following seas, forward speed

Scales are the same in all figures. Wave steepness ( $h/\lambda$ ) is the abscissa, bending moment coefficient the ordinate. The vertical scale at the left on the plot denotes wave hogging and sagging moments ( $\mu_s, \mu_H$ ). The scale to the right on each plot is the "absolute" bending coefficient ( $\mu_{HA}, \mu_{SA}$ ); that is, the origin of the wave bending coefficient scale has been translated to account for the static still water bending moment. This scale corresponds to the bending moments ordinarily obtained in the design office. The results of conventional static calculations in model length waves of various heights are shown. The numbers which label each of the lines drawn on these plots indicate the wave length to ship length ratio.

## 2. Trends of pitch and heave amplitudes with wave steepness.

A condensation similar to that for bending moments has been made of the faired lines through the pitch and heave amplitude data (Ref. 5). This condensation is shown in Figs. 35 to 50 which are arranged in the following order:

- 35 - 38 Four models, head seas, forward speed
- 39 - 42 Four models, head seas, zero speed
- 43 - 46 Four models, head seas, drifting astern
- 47 - 50 Four models, following seas, forward speed

Scales are the same in all figures. The top half of each is a plot of pitch double amplitude in degrees ( $2\theta$ ) against wave steepness and the bottom half is a similar plot of heaving amplitudes ( $2Z_o/L$ ). Lines are labeled with the applicable wave length to ship length ratio.

## 3. Cross plots of bending moments and motions.

In order to facilitate comparison between models, cross plots were made of the data in Figs. 19 to 50 for wave steepnesses of 0.04 and 0.10. The resulting plots are presented in Figs. 51 to 54. Cross-plotted moments and motions are shown for the various speed cases as follows:

- Figure 51 Head seas, forward speed
- 52 Head seas, zero speed
- 53 Head seas, drifting astern
- 54 Following seas, forward speed

At the upper left hand side of each figure cross plots of pitching amplitudes at the two wave steepnesses are shown. Heaving double amplitudes are cross-plotted in similar fashion directly below. The next plot, from left to right on each figure, shows wave sagging and hogging moments for wave steepness of 0.04. The plot immediately adjacent is of sagging and hogging moments at a wave steepness of 0.10. The plot at the far right of each figure in which the ordinate is labeled  $\mu_s^t$  and  $\mu_H^t$ , is of approximate hydrodynamic bending moments. The source of these "hydrodynamic" bending moments will be discussed subsequently.

The abscissa of each plot is wave length to ship length ratio, and notation

MODEL 2251A-V1, MARINER, PARENT  
 MODEL HEADING: 180° HEAD SEAS  
 APPROX. MODEL SPEED:  $v/\sqrt{gL} = 0.12$  to  $0.14$

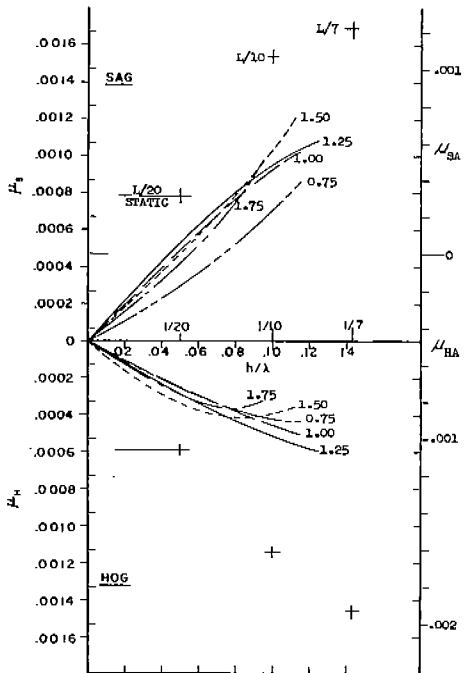


FIG. 19.

MODEL 2251A-Y2, MARINER, CARGO AT MIDSHIP  
 MODEL HEADING: 180° HEAD SEAS  
 APPROX. MODEL SPEED:  $v/\sqrt{gL} = 0.12$  to  $0.14$

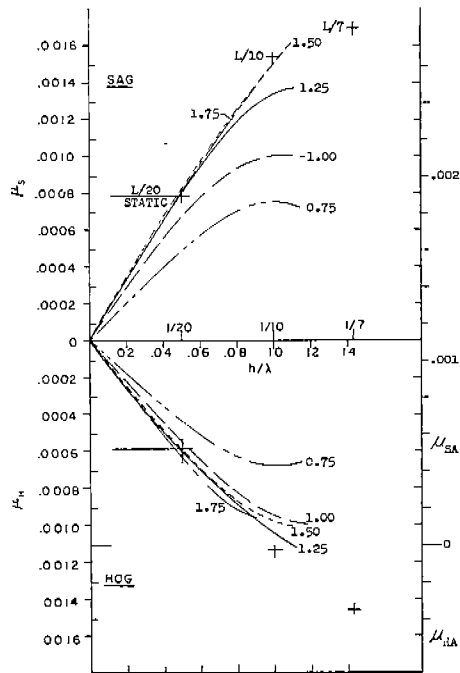


FIG. 20.

MODEL 2251A-Y3, MARINER, CARGO AT ENDB  
 MODEL HEADING: 180° HEAD SEAS  
 APPROX. MODEL SPEED:  $v/\sqrt{gL} = 0.12$  to  $0.14$

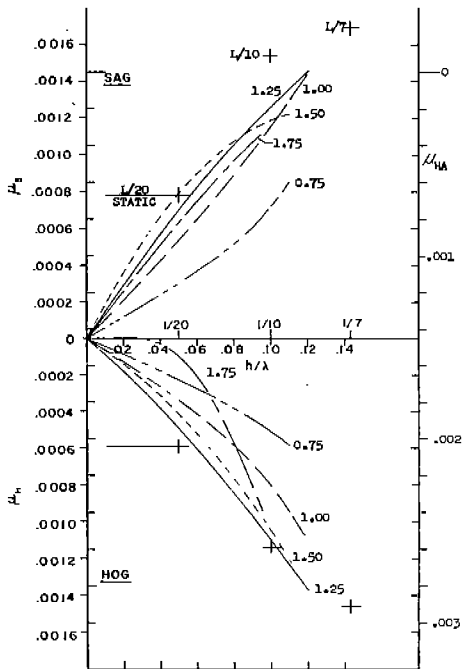


FIG. 21.

MODEL 2251B, MARINER, INCREASED FOREBOARD  
 MODEL HEADING: 180° HEAD SEAS  
 APPROX. MODEL SPEED:  $v/\sqrt{gL} = 0.12$  to  $0.14$

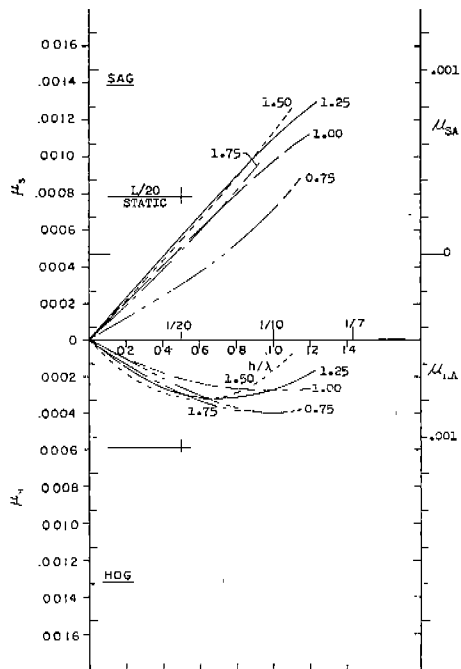


FIG. 22.

FIG. 19-22. TRENDS OF BENDING MOMENT WITH WAVE STEEPNESS.

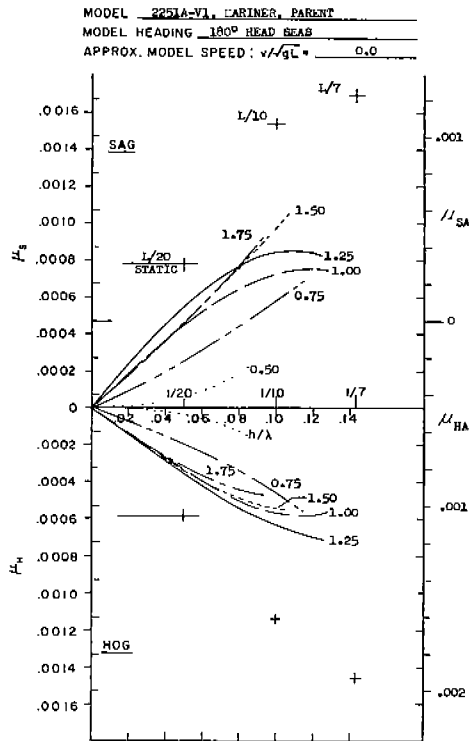


FIG. 23.

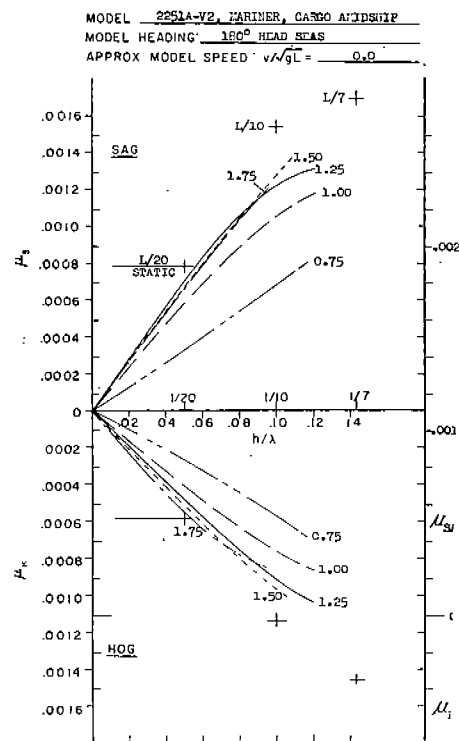


FIG. 24.

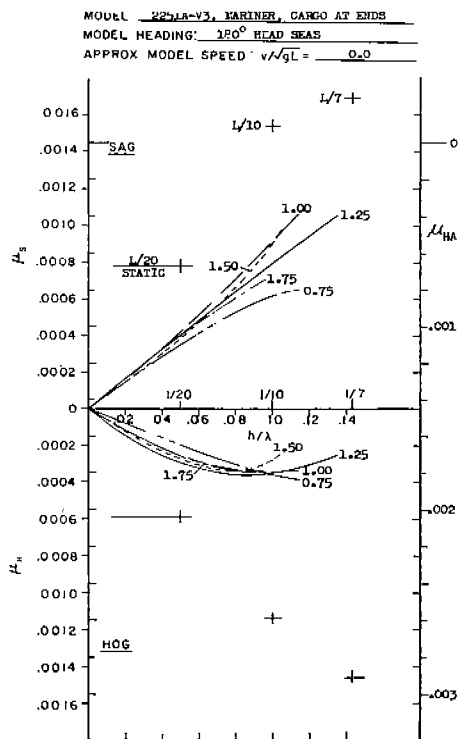


FIG. 25.

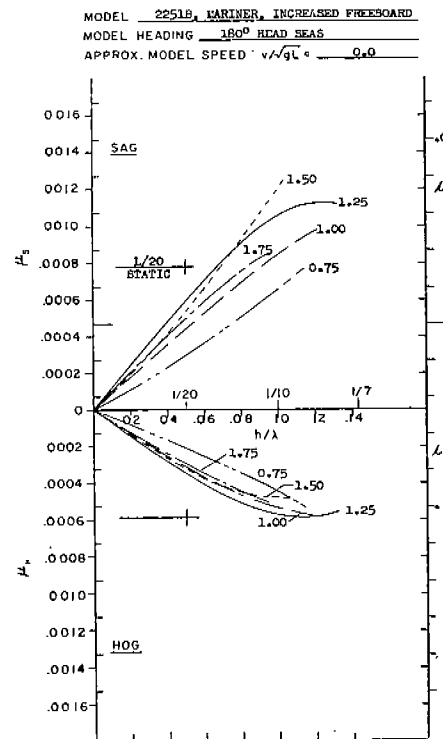


FIG. 26.

FIG. 23-26. TRENDS OF BENDING MOMENT WITH WAVE STEEPNESS.

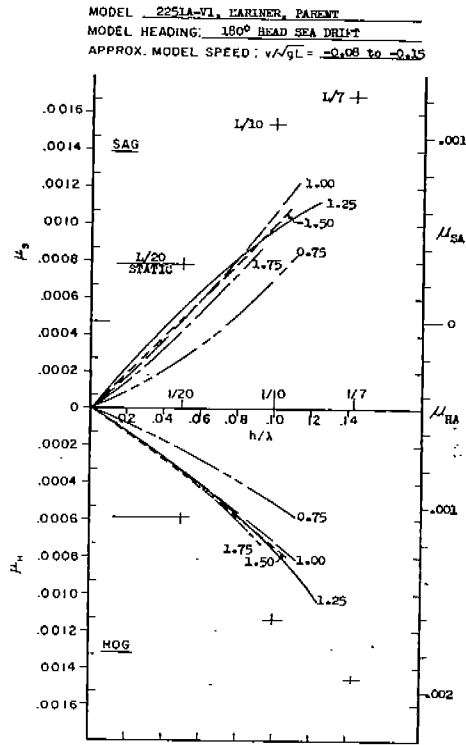


FIG. 27.

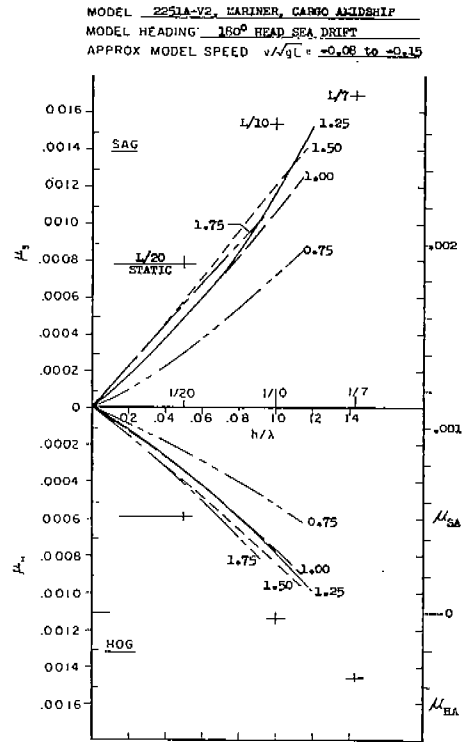


FIG. 28.

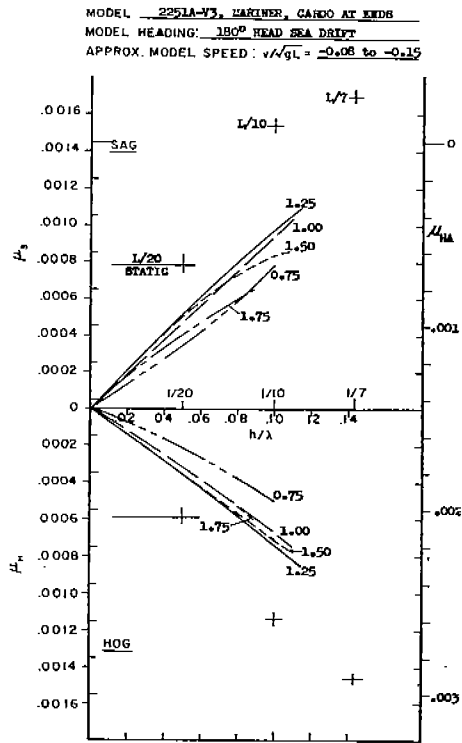


FIG. 29.

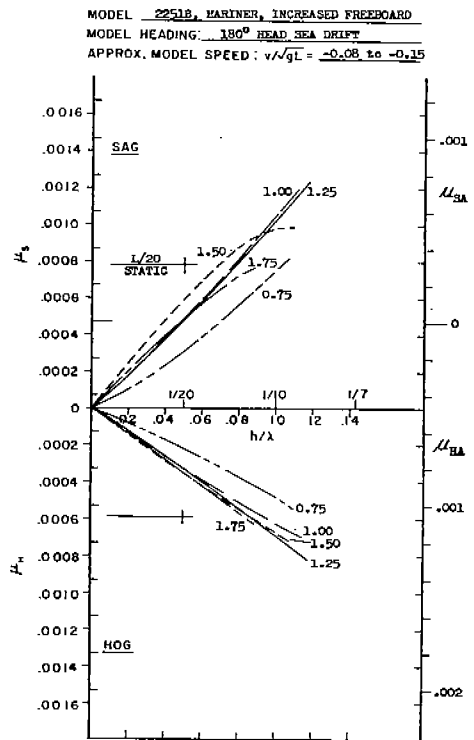


FIG. 30.

FIG. 27-30. TRENDS OF BENDING MOMENT WITH WAVE STEEPNESS.

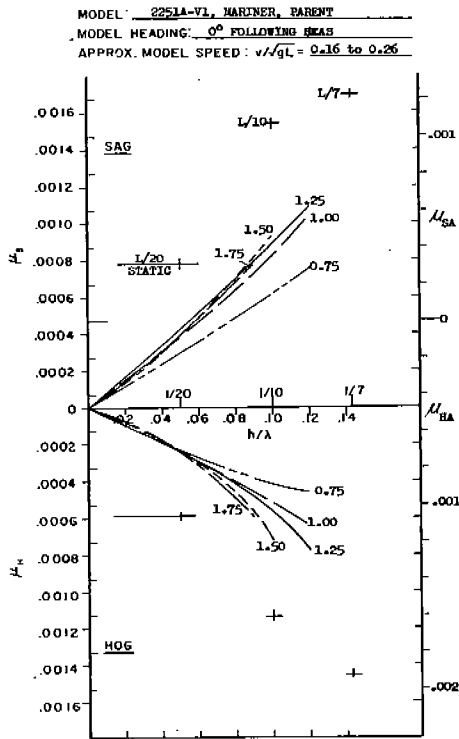


FIG. 31.

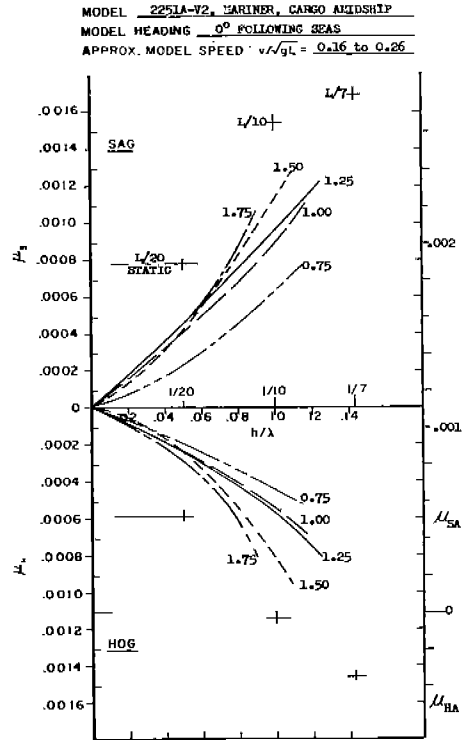


FIG. 32.

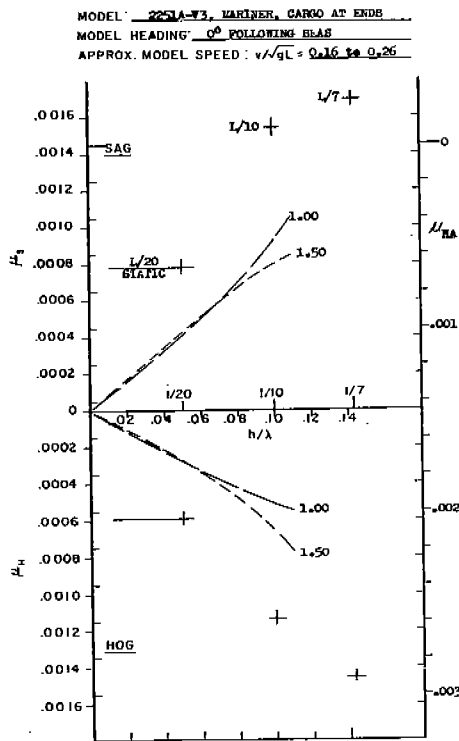


FIG. 33.

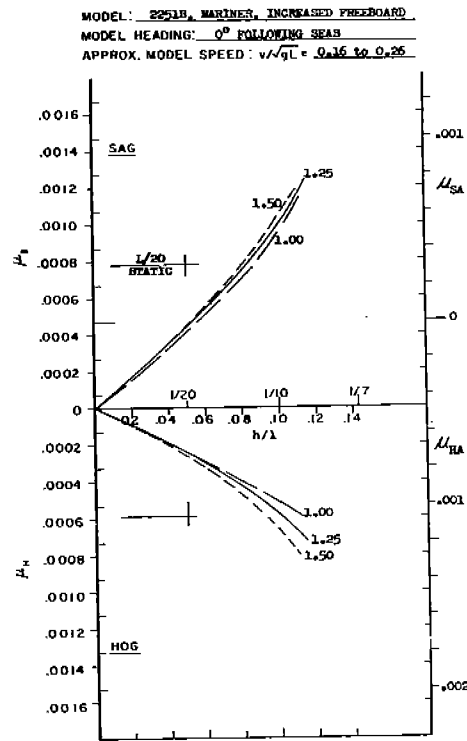


FIG. 34.

FIG. 31-34. TRENDS OF BENDING MOMENT WITH WAVE STEEPNESS.

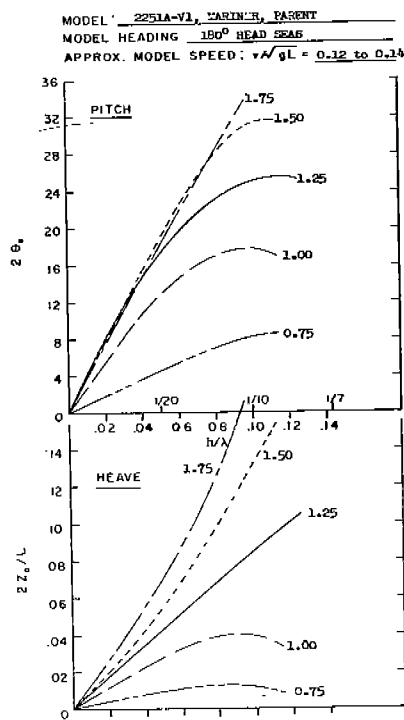


FIG. 35.

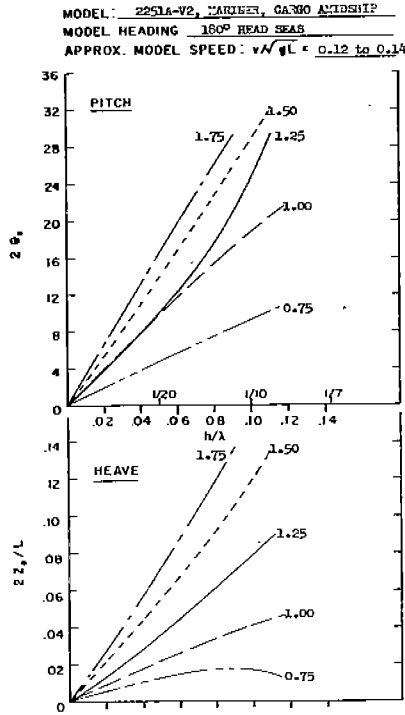


FIG. 36.

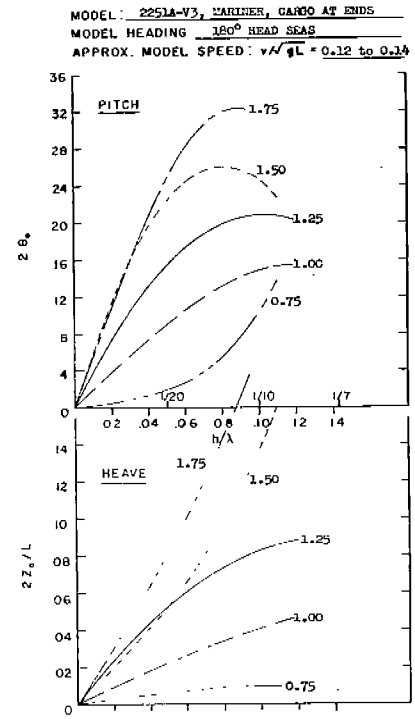


FIG. 37.

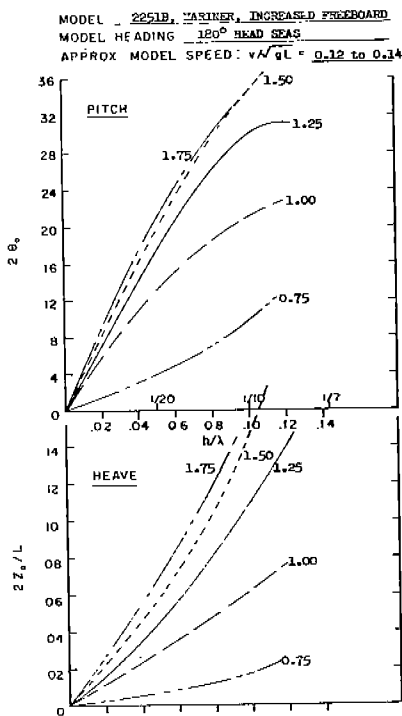


FIG. 38.

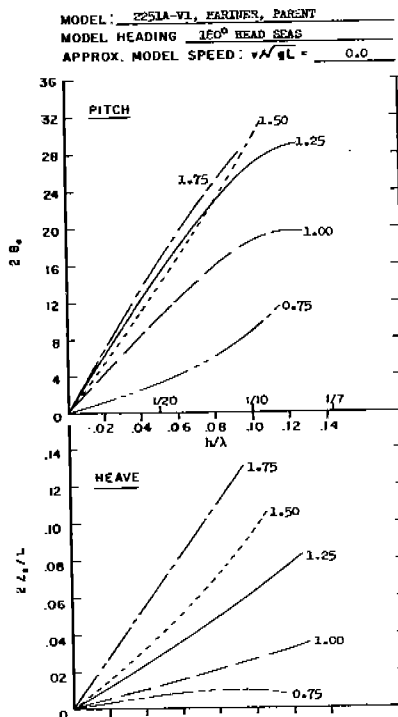


FIG. 39.

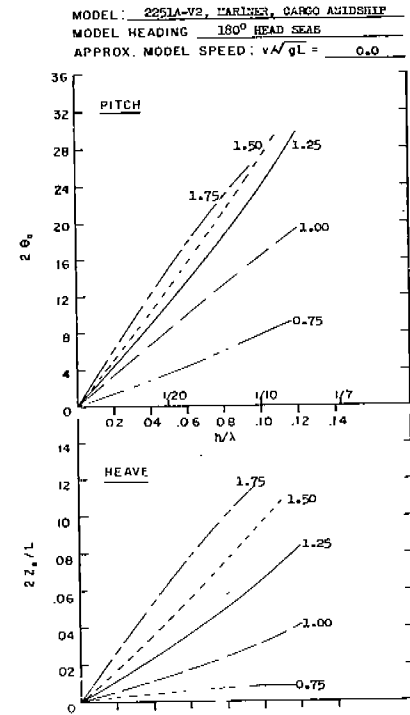


FIG. 40.

FIG. 35-40. TRENDS OF PITCH AND HEAVE AMPLITUDES WITH WAVE STEEPNESS.

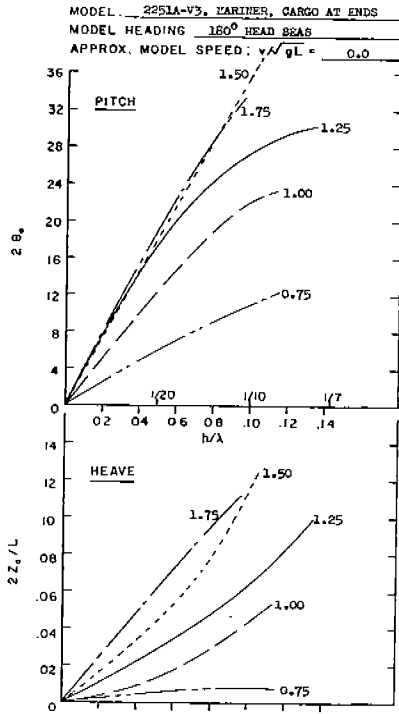


FIG. 41.

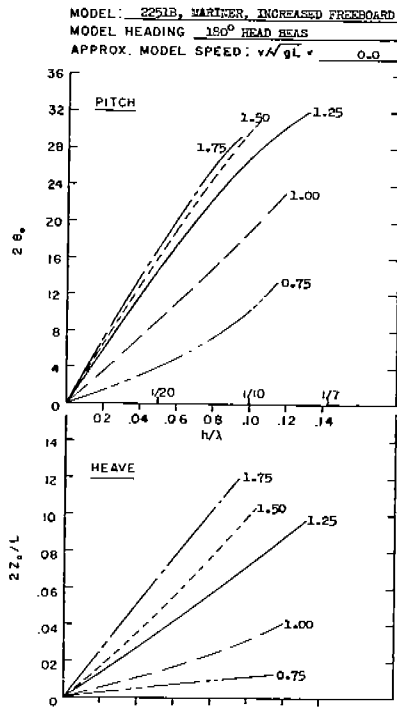


FIG. 42.

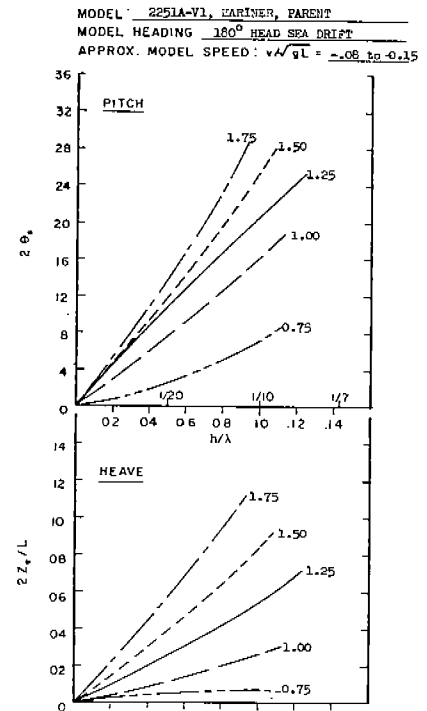


FIG. 43.

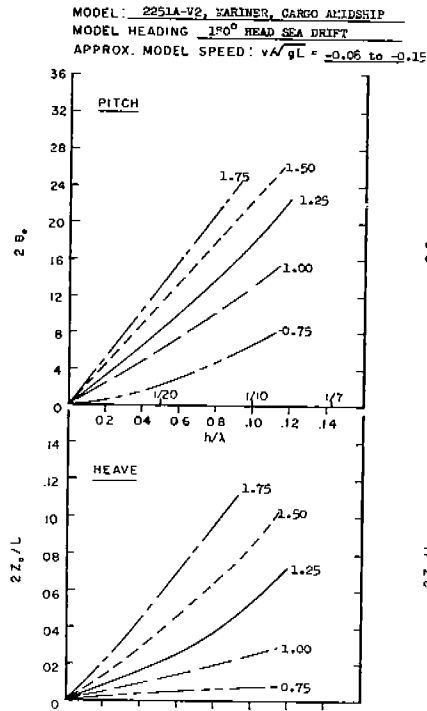


FIG. 44.

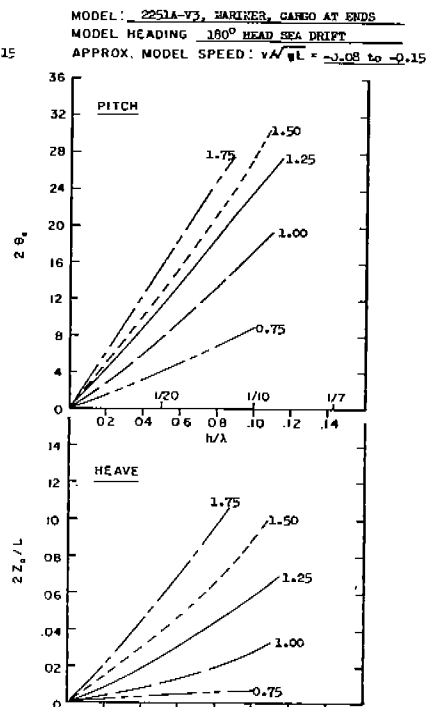


FIG. 45.

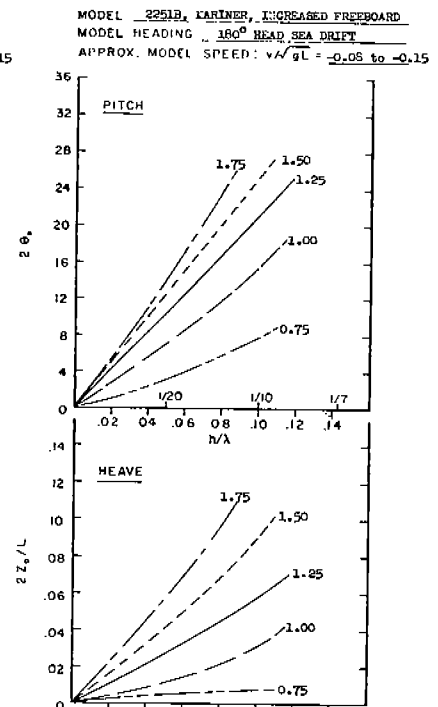


FIG. 46.

FIG. 41-46. TRENDS OF PITCH AND HEAVE AMPLITUDES WITH WAVE STEEPNESS.

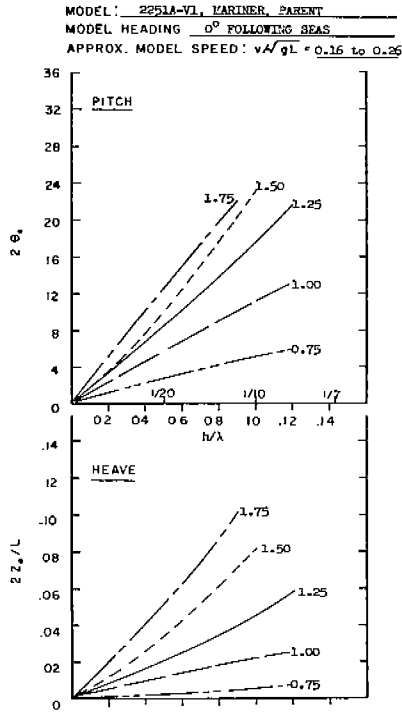


FIG. 47.

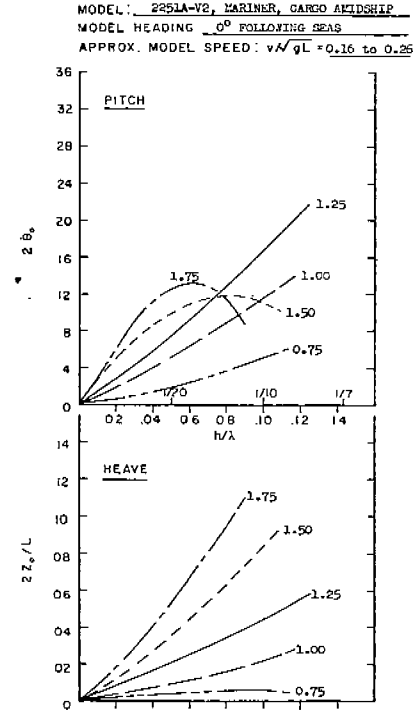


FIG. 48.

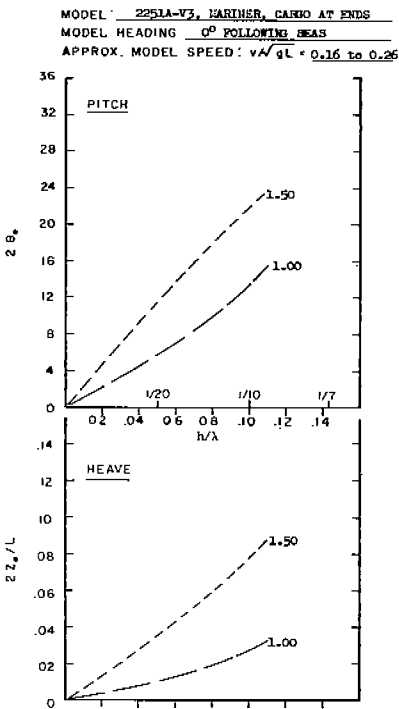


FIG. 49.

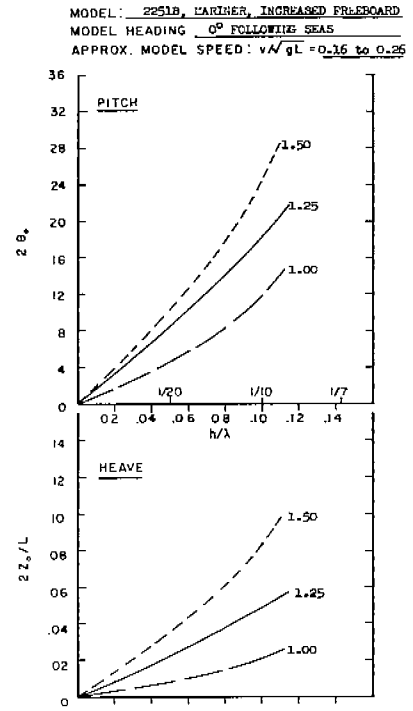


FIG. 50.

FIG. 47-50. TRENDS OF PITCH AND HEAVE AMPLITUDES WITH WAVE STEEPNESS.

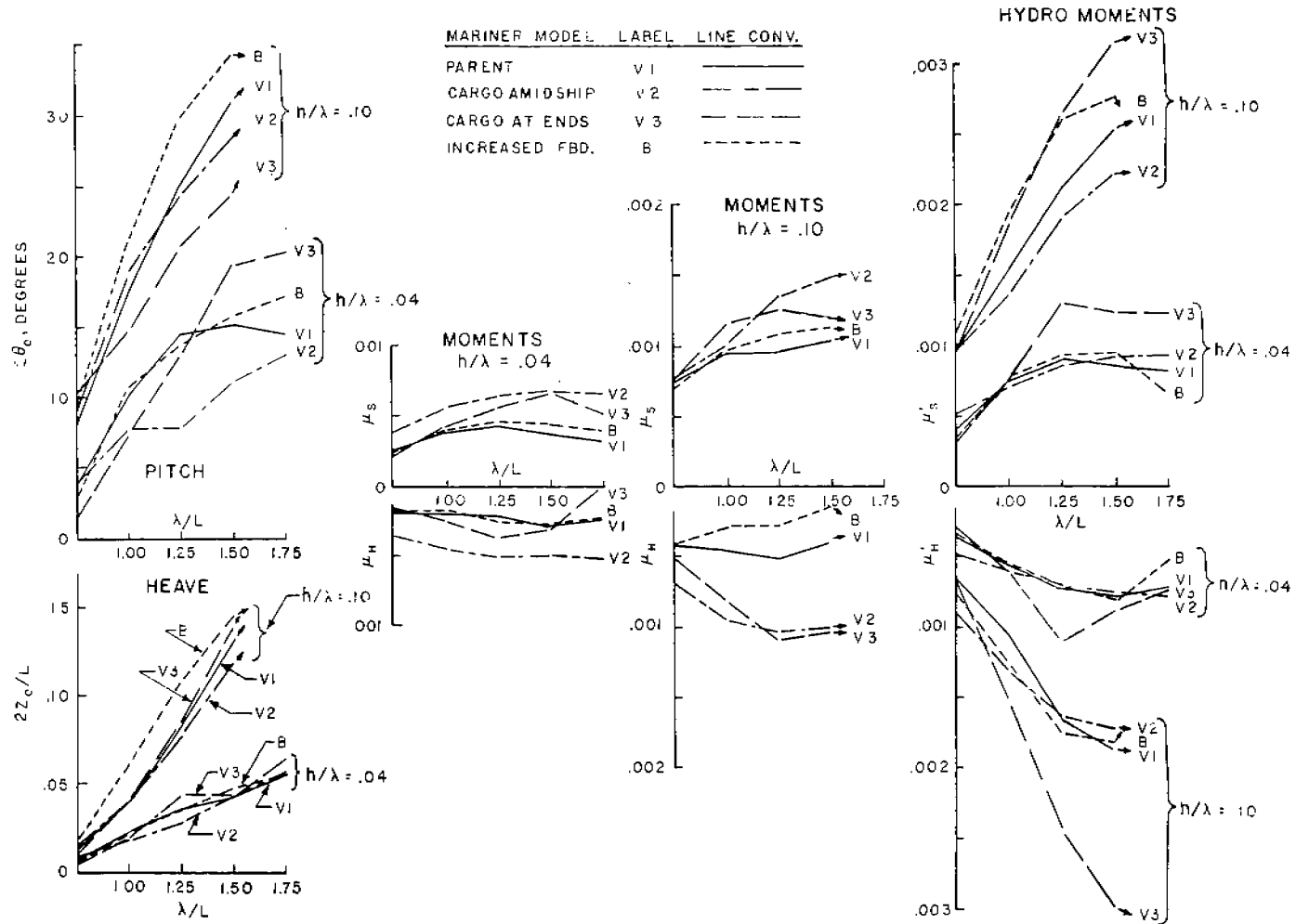


FIG. 51. CROSS PLOT OF PAIRED MOMENTS AND MOTIONS, HEAD SEA, PROUDE NO. 0.12 TO 0.14.

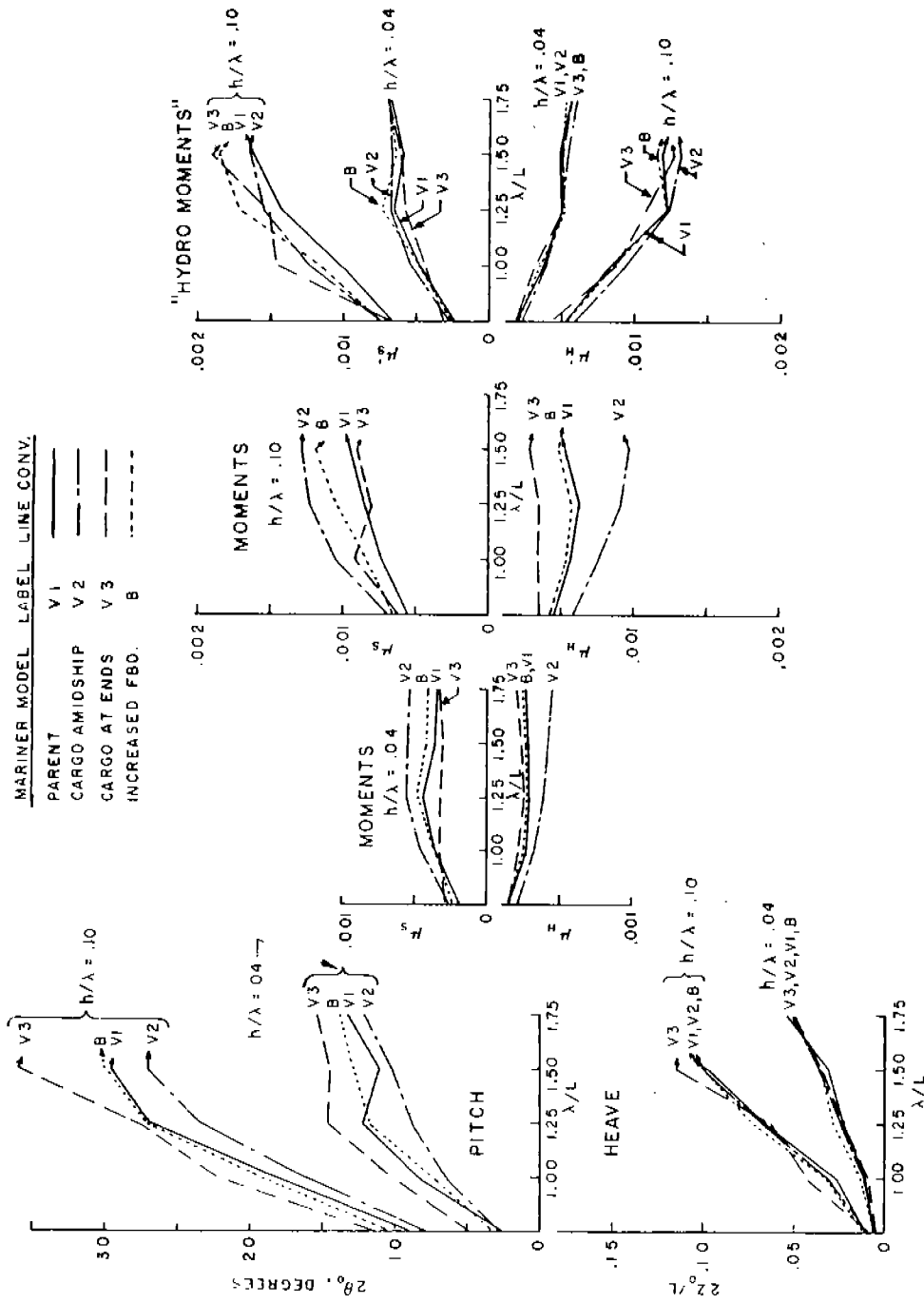


FIG. . CROSS PLOT OF FAIRED MOMENTS AND MOTIONS, HEAD SEAS, FROUDE NO. 0.0.

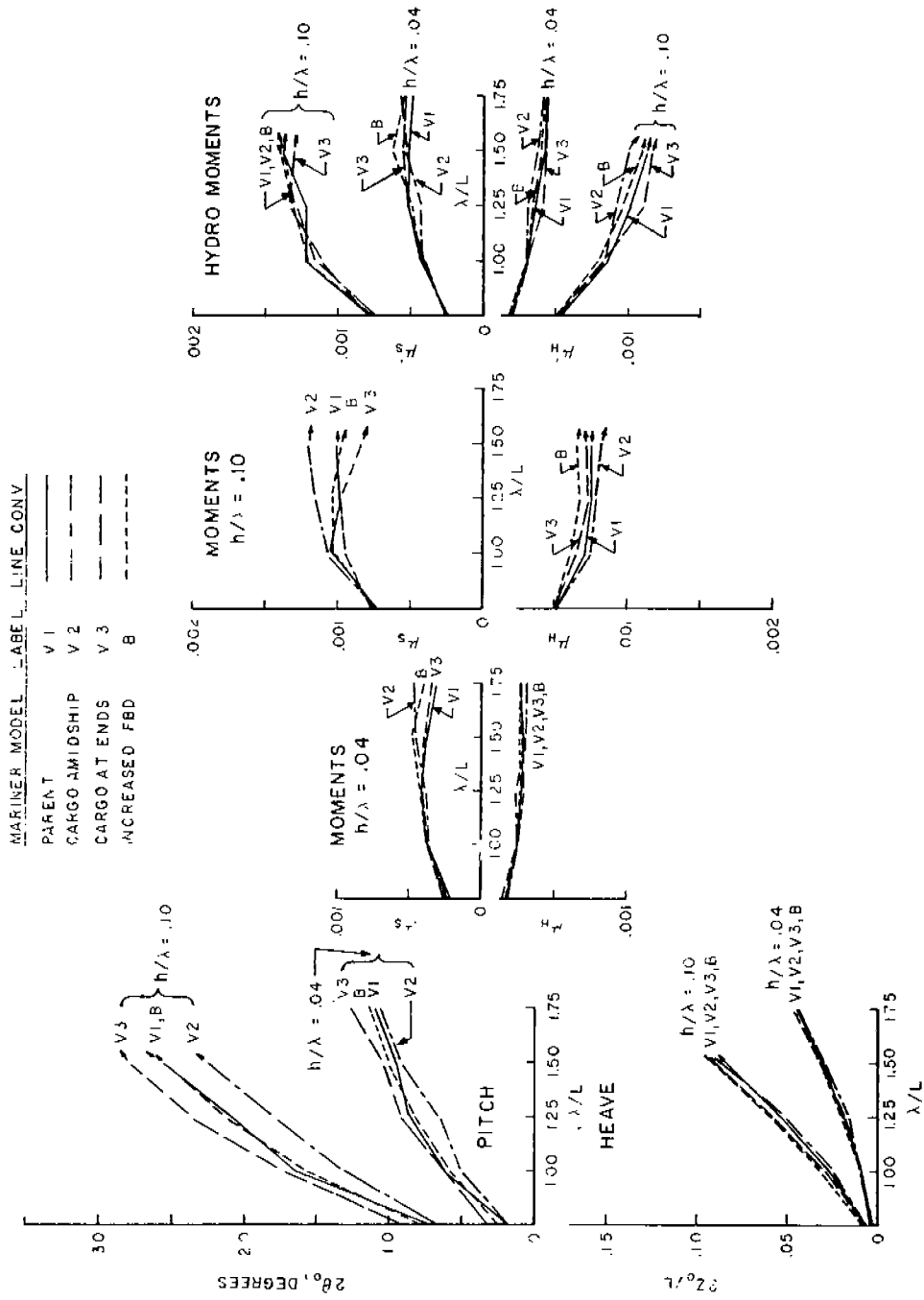


FIG. 53. CROSS PLOT OF FAIRED MOMENTS AND MOTIONS, HEAD SEAS, DRIFTING ASTERN, FROUDE NO. -0.08 TO -0.15.

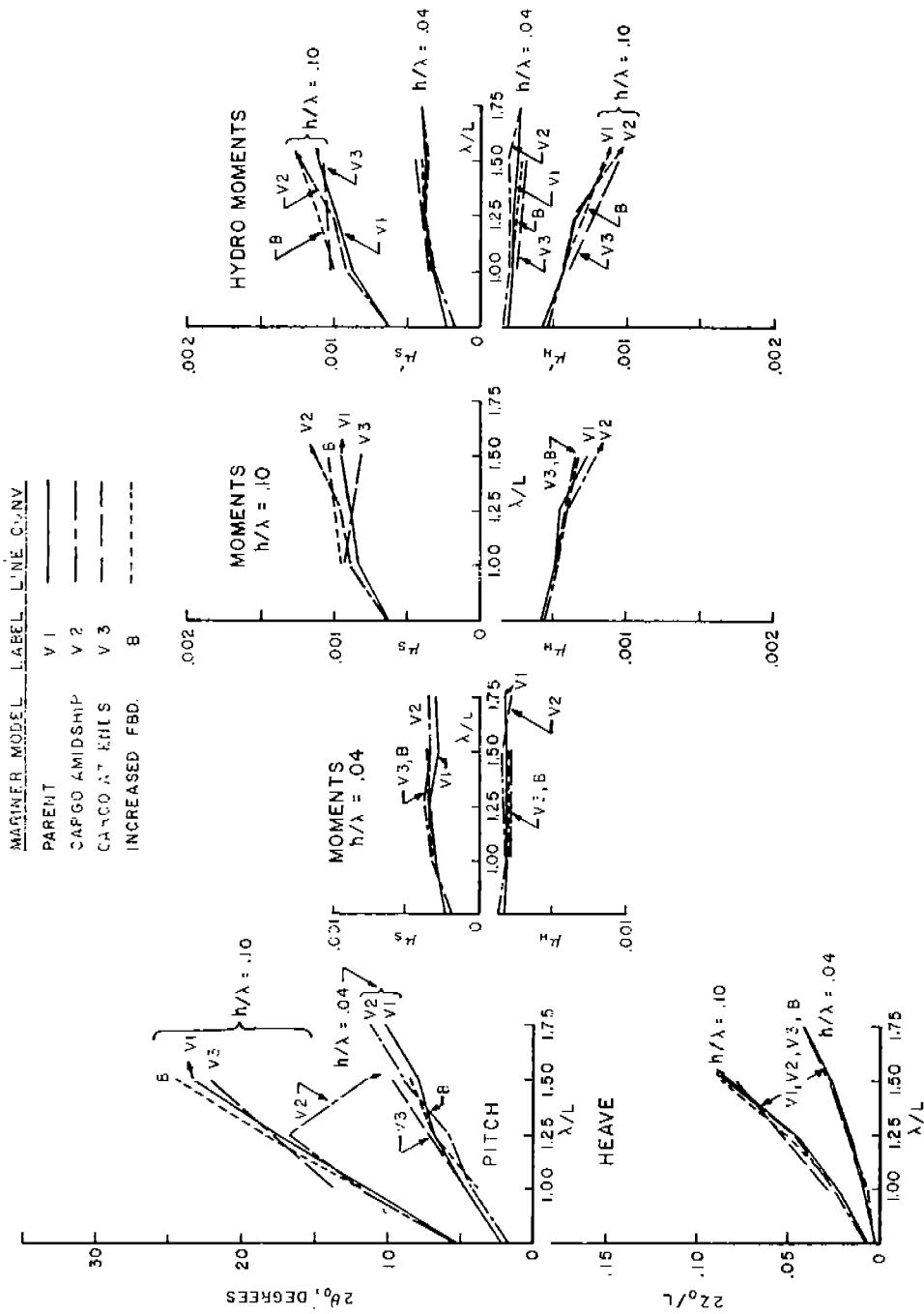


FIG. 54. CROSS PLOT OF PAIRED MOMENTS AND MOTIONS, FOLLOWING SEAS, FROUDE NO. 0.16 TO 0.26.

is the same as in Figs. 19 to 50. Arrows shown at the ends of some of the lines show the direction in which the line would go if the point on the faired curve for the next higher wave length had been plotted. In all cases where an arrow is shown the faired line through the data points for the next higher wave length did not extend to a steepness of 0.09 and was therefore not considered valid for a wave steepness of 0.10.

Line conventions denoting the four models are shown on each plot.

## ANALYSES

### A. Comparisons with Other Test Data

A question which is frequently raised is that while data presented may be consistent with itself, the possibility exists that it may not be consistent with previous data. In order to make a comparison with previous data, attention must be concentrated on results in waves of a steepness below 0.05 ( $L/20$ ). In the present work very little data were obtained in this region, but it is of interest to compare the mean slope of the fitted curves in the very low wave height region with previously obtained data. The slope of the fitted curves in this region may be used to obtain the moment coefficient ordinarily used in the presentation of bending moment data in moderate waves. That is:

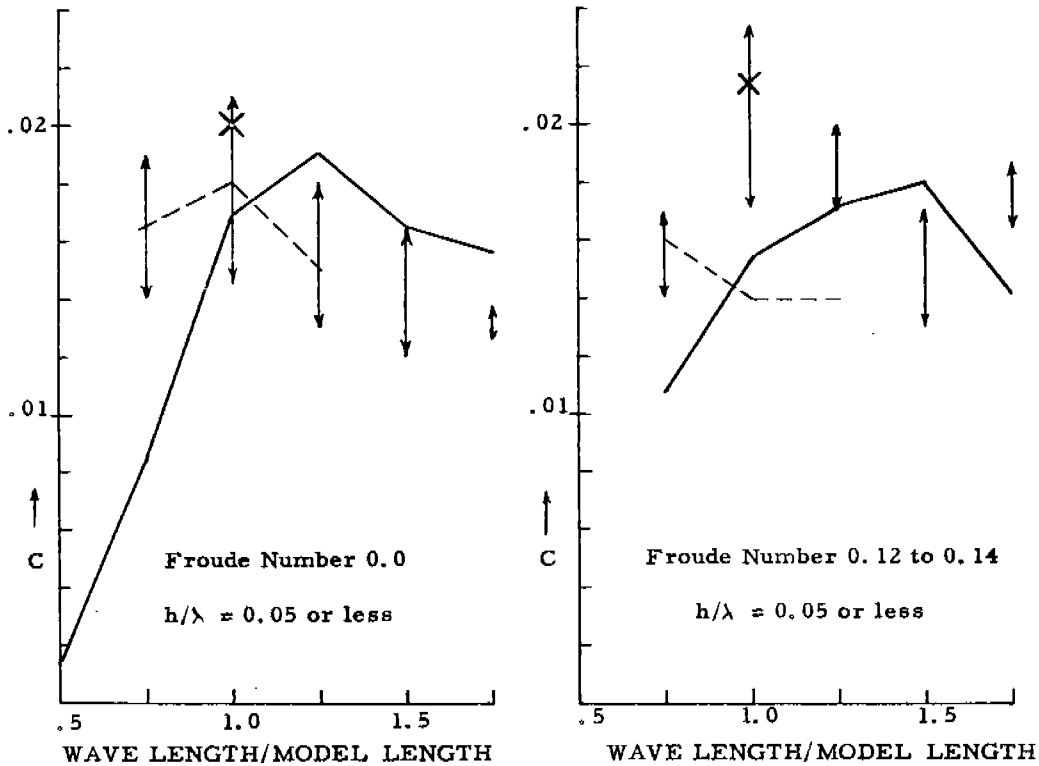
$$\mu = C(h/\lambda) (\lambda/L)$$

$$\frac{d\mu}{d(h/\lambda)} = C(\lambda/L)$$

$$C = L/\lambda \cdot \frac{d\mu}{d(h/\lambda)}$$

Since the present data is presented in terms of Hog and Sag, the sum of the slopes of the curves fitted through the test points was multiplied by  $L/\lambda$  and used as the moderate wave bending moment range coefficient. Figure 55 shows comparisons of "C" coefficients in two plots, one at zero speed and one at Froude No. = 0.12 - 0.14. The solid line in each plot shows the trend of moment coefficients derived from the fitted curves for the parent Mariner in various wave lengths. The dashed lines indicate the moment coefficients obtained for a Series 60, 0.60 block coefficient model by DeDoes, Ref. 6. This model and the parent Mariner are similar in hull form and weight distribution and only one percent different in block coefficient. Accordingly, there should be reasonably close agreement between the two sets of results. The agreement is quite good in 1.0L waves at both speeds; greater differences occur at the other wave lengths. However, it is believed a reasonable degree of agreement has been demonstrated, keeping in mind that the Mariner results were derived from curves fitted through a region in which few data were obtained.

Figure 55 also shows moment coefficients for a Series 60, 0.68 block coefficient model (Ref. 7) and for the 0.74 block coefficient, T-2 tanker models tested by six investigators in different towing tanks (Ref. 8). These results are generally higher than the Mariner coefficient, particularly in 1.0L waves. This is to be expected since Ref. 7 demonstrated that wave bending moment increases as the block coefficient is raised. Thus a second, less direct but nevertheless reasonable, check on the Mariner results is obtained. It is also important to note that the differences between range coefficients found for the T-2 tanker model by six investigators in different towing tanks are of the same order as the differences between the Series 60 Model (Ref. 6) and the Mariner.



KEY AND SOURCE OF DATA

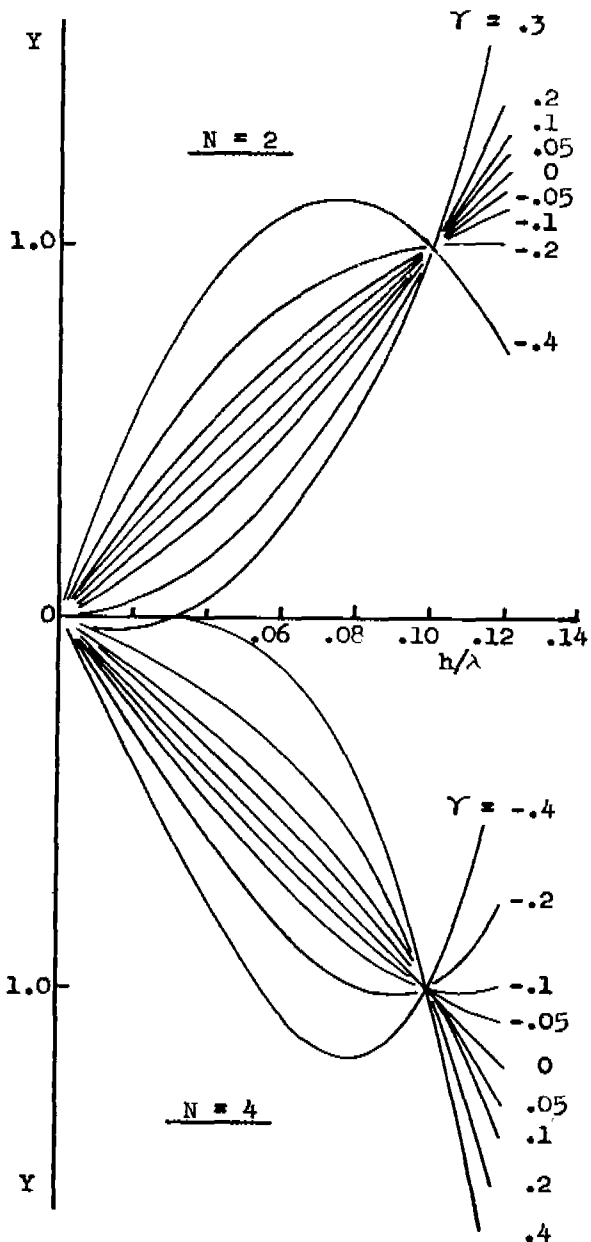
- Model 2251 A-V1, Parent Mariner,  $C_B = 0.61$
- - - - Series 60,  $C_B = 0.60$ , "Experimental Determination of Bending Moments for Three Models of Different Fullness in Regular Waves," DeDoes, J. C., Delft 1960.
- × Series 60,  $C_B = 0.68$ , "Effect of Speed and Fullness on Hull Bending Moments in Waves," Dalzell, J., Davidson Lab. 1959
- ↑ ↓ T-2 Tanker,  $C_B = .74$ , Range of Results Obtained by Six Investigators, Report of Committee on Wave Loads, International Ship Structures Congress, Glasgow 1961.

FIG. 55. COMPARISON OF BENDING MOMENT RANGES MEASURED IN THE MARINER WITH OTHER TEST RESULTS.

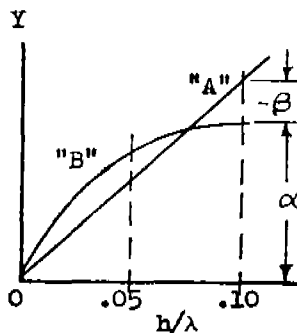
B. Classification of Trends

Even though the presentation of trends of bending moments and motions with wave steepness in Figs. 19-50 compresses the basic results five fold, it is still rather difficult to keep track of the differences in trend of bending moment and motions with wave steepness. Therefore an approximate numerical classification of the shape of the lines in Figs. 19-50 were made. Figure 56 summarizes the definition of the numerical criterion finally adopted and shows plotted examples.

The sketch at the right hand side of Fig. 56 illustrates the criterion, ( $\gamma$ ) and the method of computation. In order to classify the shape of curve (B) in that sketch, a straight line through the origin was first fitted to curve (B) over a region of wave steepness between 0.05 and 0.10. A least squares fitting technique was used.



DEFINITION OF  $\gamma$



STRAIGHT LINE "A"  
 A LEAST SQUARE FIT  
 TO CURVE "B" OVER THE  
 REGION DEFINED BY:

$$.05 \leq h/\lambda \leq .10$$

THEN:

$$\gamma = \beta/\alpha$$

FOR CURVES OF FORM:

$$Y = a(h/\lambda) + b(h/\lambda)^N$$

$$\gamma \approx \frac{N}{\left(\frac{a}{b \cdot 10^{-N}} + 10\right)}$$

FIG. 56. NUMERICAL CLASSIFICATION OF FITTED CURVES: DEFINITION AND EXAMPLES.

The difference between curve (B) and the fitted straight line (A) at a wave steepness of 0.10 was then evaluated ( $\beta$ ). If this difference is negative (See Fig. 56) the curve B is convex upward, if the quantity  $\beta$  is positive, curve B is concave upwards. The straight line was fitted between wave steepnesses of 0.05 and 0.10 primarily because this is the region of wave steepness where actual data was obtained in all cases. The quantity  $\beta$  is also almost directly proportional to the difference between the slope of curve (B) at a wave steepness of zero and the slope at a wave steepness of 0.10. This fact strengthens its use as a criterion.

It was felt that  $\beta$  should be normalized to account for variations in magnitude of the moments and motions, and it was therefore divided by the ordinate of the

fitted curve (B) at a wave steepness of 0.10 ( $\alpha$ , Fig. 56), to yield the numerical criterion,  $\gamma$ . For curves of the analytic form used for the computer fitting of the test data,  $\gamma$  is simply evaluated with the coefficients in the equation. The left hand side of Fig. 56 shows examples of curves with different  $\gamma$  criteria. The abscissa of this plot is wave steepness, the ordinate can be either bending moments or motions. Two families of curves are plotted, the top family for an exponent of the second term in the equation equal to 2; the bottom family for an exponent of 4. The  $\gamma$  value for each curve is noted and it can be seen that the differences in shape between curves for  $N = 4$  and  $N = 2$  for the same value of  $\gamma$  are relatively small. It was seen that the percentage differences in ordinates between curves with  $\gamma$  values differing by 0.10 or less are something like the percentage scatter of data points shown in Ref. 5. It was therefore felt that it was pointless to present results from the numerical classification in fine numerical detail.

A value of  $\gamma$  was computed for each mean line shown in Figs. 19-50. The results were divided into five classes:

Class ++:	Curves with $\gamma$ greater than 0.15
Class + :	" " " between +.15 and +.05
Class 0 :	" " " " +.05 and -.05
Class - :	" " " " -.05 and -.15
Class --:	" " " less than -.15

If a curve falls in the third category one could almost call it a straight line. Curves in the second or fourth categories show the beginnings of a trend with wave steepness. If a curve falls in the first or fifth categories a definite trend is shown.

Results of the computations and classifications are summarized in Tables IV and V where results are shown separately for sagging moment, hogging moment, pitch amplitudes and heaving amplitudes as well as the approximate hydrodynamic sagging and hogging moments to be discussed subsequently. It may be noted that no computations were made for wave lengths of  $0.5L$  in the head sea case nor for  $0.75L$  in the following sea case.

Table IV applies to the weight distribution investigation, Table V to the freeboard investigation.

### C. Maximum Bending Moments in Waves of Fixed Height

The cross plots of Fig. 51-54 are made on the basis of constant wave steepness. It was felt of interest to display the moments in extreme waves of constant height. The reason for this distinction was that the highest wave developed in the model tests is about 100 feet high to Parent Mariner scale. It is unclear whether such an extreme wave does occur in deep water with any measurable frequency and it was felt that somewhat different conclusions might be drawn from cross plots of bending moments for constant wave height than are drawn from cross plots for constant wave steepness. Figures 57, 58 and 59 are cross plots of the faired bending moments of Fig. 19-34 for waves of a height equal to 10% of the ship length, (full scale about 50 ft. in height). An exception was made in the case of the  $0.75L$  waves where the values for a wave steepness of 0.10 are shown. (This was done in order to avoid using points from an extrapolation of the curves fitted to the data.) Only the results for the three practical speed-heading conditions are shown. Results for all models are shown in each plot.

TABLE IV. WEIGHT DISTRIBUTION INVESTIGATION - CLASSIFICATION OF TRENDS WITH WAVE STEEPNESS OF MOMENT AND MOTIONS.

Speed, Heading	$\lambda/L$	Sagging Moment		Hogging Moment		Pitch		Heave		Hydro. Sag		Hydro. Hog	
		Cargo Amidship	Parent	Cargo at Ends	Cargo Amidship	Parent	Cargo at Ends	Cargo Amidship	Parent	Cargo at Ends	Cargo Amidship	Parent	Cargo at Ends
0.12 to 0.14, 180°	0.75	-	+	+	-	-	0	0	-	+	-	-	0
	1.00	-	0*	0*	-	0	0	0	-	+	0*	0*	0
	1.25	-	0*	0*	-	0	0*	0	-	+	0*	0*	0
	1.50	0	0*	-*	-	-	+	0	-	+	0*	0*	0
	1.75	0	+	0*	-	-	+	0	-	+	0*	0*	0
0.0, 180°	0.75	0	0	0	0	+	0	0	+	0	0	0	0
	1.00	0	-	0*	0	-	0	0	-	0	0	0	0
	1.25	-	0	0*	0	-	-	0	-	0	0	0	0
	1.50	0	0	+	0	-	0	0	+	0	0*	0	0
	1.75	0	0	0	-	-	0	0	+	0	+	0	0
-0.08 to -0.15, 180°	0.75	+	+	0	0	0	0	+	0	0	0	0	0
	1.00	0	0	0	0	0	0	0	0	0	0	0	0
	1.25	+	0	0	0	0	0	0	0	0	0	0	0
	1.50	0	0	-	0	0	0	0	0	0	0	0	0
	1.75	-	0	0	+	+	0	0	0	0	0	0	0
0.16 to 0.26, 0°	1.00	0	0	0	0	0	0	+	+	0	0	0	0
	1.25	0	0	ND	+	+	ND	0	0	ND	0	+	+
	1.50	+	+	0	++	+	+	-	0	0	+	+	ND

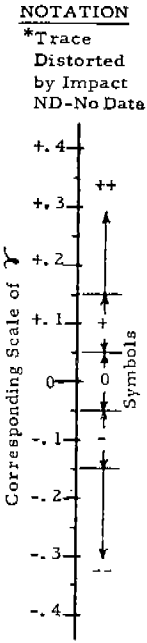
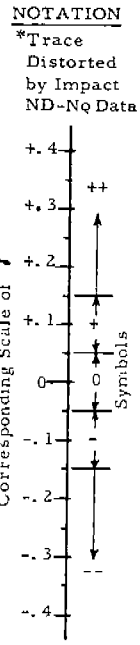


TABLE V. FREEBOARD INVESTIGATION - CLASSIFICATION OF TRENDS WITH WAVE STEEPNESS OF MOMENT AND MOTIONS.

Speed, Heading	$\lambda/L$	Sagging Moment		Hogging Moment		Pitch		Heave		Hydro. Sag		Hydro. Hog	
		Parent	Increased Freeboard	Parent	Increased Freeboard	Parent	Increased Freeboard	Parent	Increased Freeboard	Parent	Increased Freeboard	Parent	Increased Freeboard
0.12 to 0.14, 180°	0.75	+	+	-	-	-	+	-	+	0	+	-	0
	1.00	0*	0*	0	-	-	+	-	0	0*	0*	-	0
	1.25	0*	0*	0	-	-	+	-	0	0*	0*	-	0
	1.50	0*	0*	0	-	-	+	-	0	0*	0*	-	0
	1.75	+	0	-	-	-	+	-	+	+	0*	0*	0
0.0, 180°	0.75	0	0	+	0	+	+	+	0	0	0	0	0
	1.00	-	0	-	+	-	0	+	-	0	0	0	0
	1.25	0	-	-	+	-	0	0	0	0	0	0	0
	1.50	0	0	-	0	0	0	0	+	0	0	0	0
	1.75	0	+	-	0	+	0	0	0	0	0	0	0
-0.08 to -0.15, 180°	0.75	+	+	0	0	0	+	+	0	0	0	0	0
	1.00	0	0	0	0	0	0	0	0	0	0	0	0
	1.25	0	0	0	0	0	0	0	0	0	0	0	0
	1.50	0	-	0	0	0	0	0	0	0	0	0	0
	1.75	0	-	+	0	+	0	0	0	0	0	0	0
0.16 to 0.26, 0°	1.00	0	+	0	0	0	+	0	+	0	+	0	0
	1.25	0	+	+	+	0	0	0	0	0	+	+	+
	1.50	+	+	+	+	0	+	+	+	ND	0	ND	+



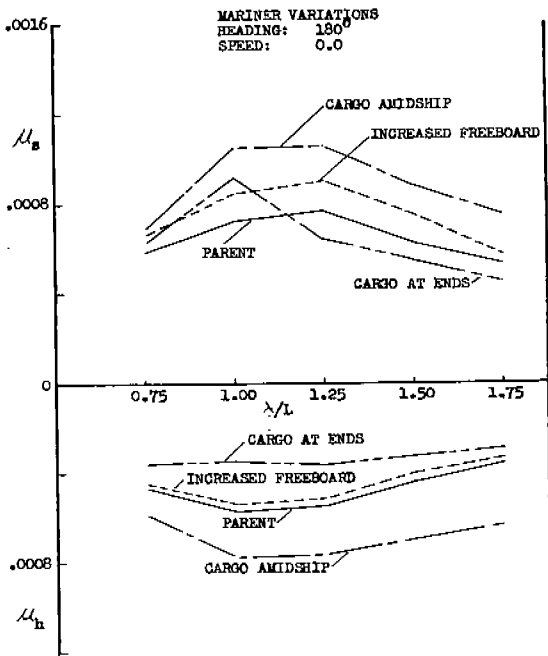


FIG. 57.

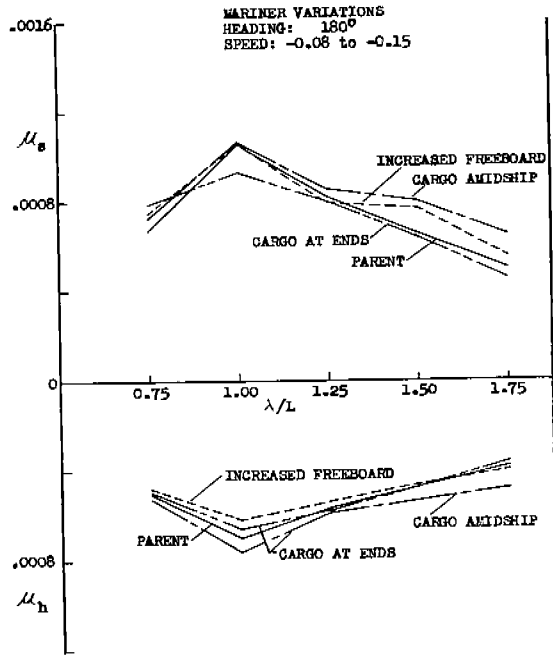


FIG. 58.

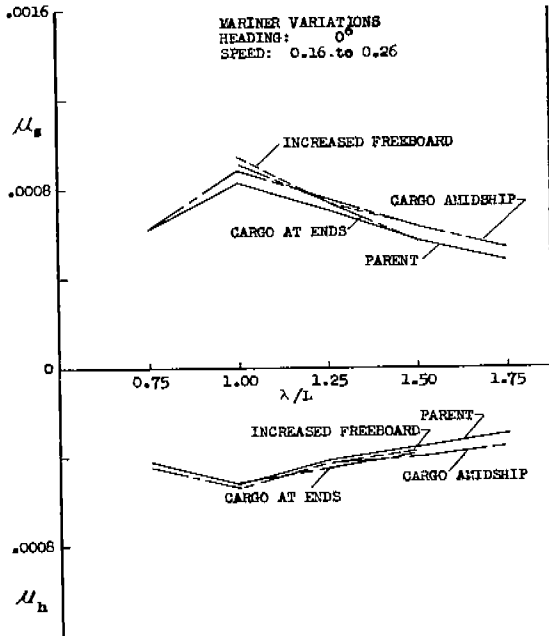


FIG. 59.

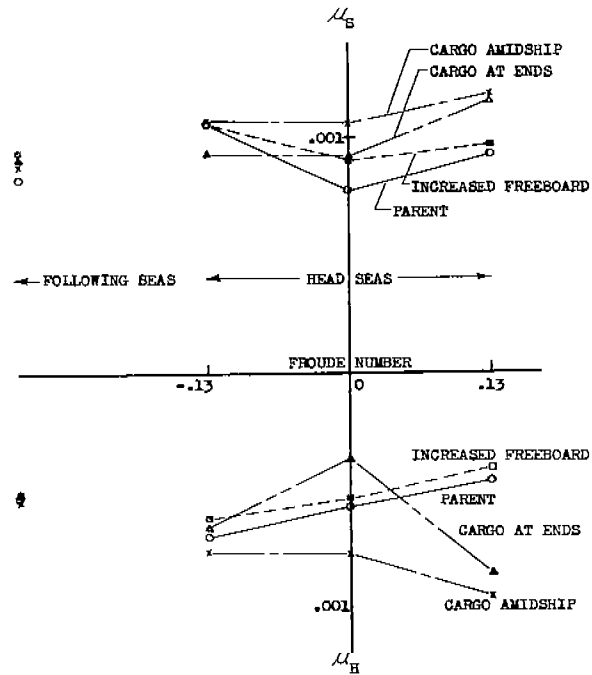


FIG. 57-59. CROSS PLOT OF FAIRED BENDING MOMENTS IN L/10 WAVES OF VARIOUS LENGTHS.

FIG. 60. VARIATIONS WITH SPEED AND HEADING OF MAXIMUM MOMENT IN L/10 WAVES OF ANY LENGTH.

It was also felt of interest to display the approximate variation with speed of the maximum moment in waves 10% of the ship length in height. This has been done in Fig. 60 where the maximum moments shown in Figs. 57-59 are plotted according to speed. Points for the maximum moments in head seas at forward speed were evaluated directly from Figs. 19 to 22. Points are connected by straight lines in the head sea cases.

#### D. Approximate Hydrodynamic Bending Moments

Since bending moments arise both as a result of the integration of water pressures and by virtue of acceleration of the mass of the model or ship, it was of interest in a first analysis to separate the hydrodynamic moment from the total measured moment. In so doing, various approximations were made in order to allow an approximate treatment of the mass of data obtained in this project rather than detailed study of fewer cases. The derivation of the moment due to accelerations of the model is shown in the Appendix. In general, the moments due to the acceleration of model mass in the forebody are unequal to the moments produced by acceleration of the model mass in the aft body. Therefore the average of the moments in the forebody and afterbody due to acceleration of mass was computed. The final approximation to the average moment due to acceleration is as follows:

$$\begin{aligned} \bar{M}_{FA} = & \left[ A_2 \omega_e^2 (2Z_o/L) \cos \delta + C_2 \omega_e^2 (2\theta_o) \cos \epsilon \right] \cos \omega_e t \\ & + \left[ A_2 \omega_e^2 (2Z_o/L) \sin \delta + C_2 \omega_e^2 (2\theta_o) \sin \epsilon \right] \sin \omega_e t \end{aligned} \quad (\text{Appendix Eq. 14})$$

where:

- $(2Z_o/L)$  = heaving double amplitude, non-dimensional
- $(2\theta_o)$  = pitching double amplitude, degrees
- $\delta, \epsilon$  = phase lags of motions following bending moment
- $\omega_e$  = wave encounter frequency
- $t$  = time
- $A_2, C_2$  = coefficients

The coefficients  $A_2$  and  $C_2$  involve only physical parameters of the models.  $A_2$  is proportional to the average of the mass moments about amidships forward and aft.  $C_2$  involves the difference of the mass moments of inertia about amidships forward and aft, and a product of model LCG and LCG's of forebody and afterbody (see Appendix).  $\bar{M}_{FA}$  was divided by the quantity  $(\rho g L^3 B)$  to non-dimensionalize. It was then evaluated for all the model, speed, heading and wave length combinations in the test program except those involving the zero speed following sea condition or the 0.50L wave length. The faired mean lines through the motions test data were used and results were calculated for values of wave steepness from 0.02 to 0.12 in steps of 0.02.

Since the expression is a harmonic function with a phase lag relative to the maximum sagging moment, the four terms of this equation were evaluated separately. An inspection of the results showed, (1) that the sum of the two first terms (those multiplying  $\cos \omega_e t$ ) was always negative, (2) that the sum of the last two terms (multiplying  $\sin \omega_e t$ ) was usually small relative to the sum of the first two terms, (3) that the second term of the equation (involving pitching amplitude) was normally

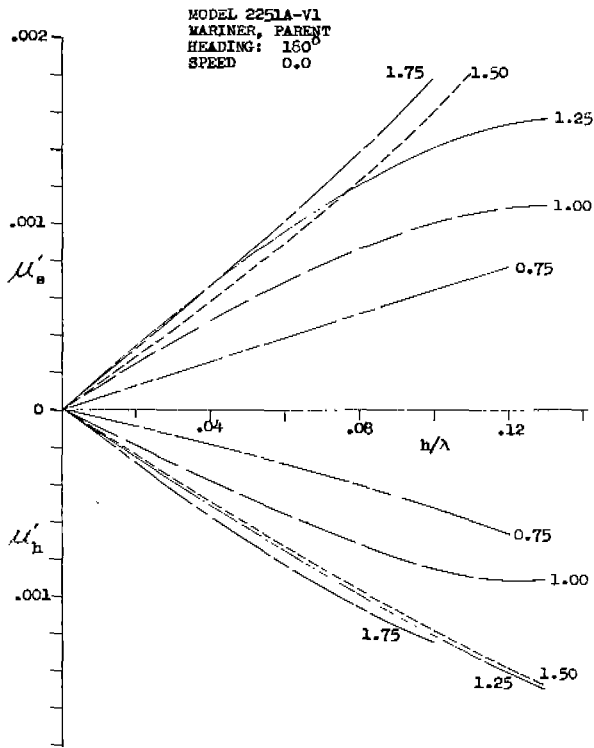


FIG. 61.

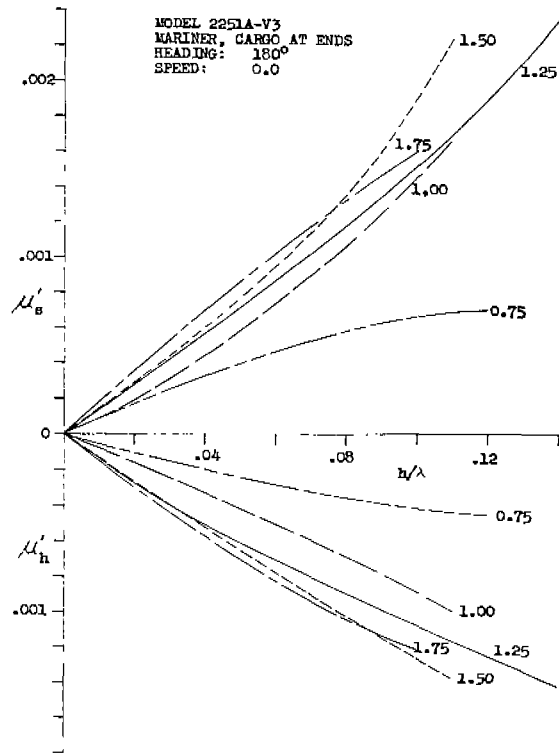


FIG. 62.

FIG. 61-62. APPROXIMATE HYDRODYNAMIC MOMENTS.

small relative to the first term. In order to derive an approximate hydrodynamic bending moment it was necessary to subtract the average bending moment due to acceleration from the measured moments. In order to do this with the data at hand and without going back to the original test record, it was necessary to assume that the bending moment was co-sinusoidal. A vector subtraction of the foregoing expression was partially performed under the above assumption. It was found that the differences between a vector subtraction and a subtraction of the sum of the first two terms from the sagging and hogging moment amplitudes were less than 5% of the total in all, but about 10% of all the cases computed. (In this last 10% of the computations the differences were at worst 10%.) Thus, instead of assuming co-sinusoidal bending moments and doing a vector subtraction, an approximate hydrodynamic sagging and hogging moment was obtained by subtracting the sum of the first two terms of the above equation from the measured sagging and hogging amplitudes. Since the sum of the first two terms of  $\bar{M}_{FA}$  is always negative, the hydrodynamic moment is always larger than the measured moment. Because of the definition of the phases  $\delta$ , and  $\epsilon$ , this process is similar to subtracting the moments due to acceleration computed at the time of maximum sag or hogging moment from the measured sagging or hogging moment. The expression for the approximate hydrodynamic sagging and hogging moments is shown below:

$$\mu'_S = \mu_S - \bar{M}_{RE}/\rho g L^3 B$$

$$\mu'_H = \mu_H - \bar{M}_{RE}/\rho g L^3 B$$

where:

$$\bar{M}_{RE} = A_2 w_e^2 (2Z_o/L) \cos \delta + C_2 w_e^2 (2\theta_o) \cos \epsilon$$

Figures 61 and 62 show examples of the approximate hydrodynamic bending moment plotted to a base of wave steepness.

It is proper to compare Fig. 61 with Fig. 23, and while the scales are slightly different, the impression was obtained that the hydrodynamic moments show a smaller departure from a straight line trend with wave steepness than do the measured moments. Somewhat the same conclusion was drawn from a comparison of Fig. 62 with Fig. 25. Since the curves of "Hydrodynamic" moments appeared reasonably well behaved, a numerical approximation to the trend classification criterion ( $\gamma$ ) was devised and this computation was done for all of the resulting curves of hydrodynamic bending moments versus wave steepness. The results were classified as were the results from the calculation for the measured moments and are summarized in Tables IV and V under the headings Hydro Sag, and Hydro Hog. Cross plots of these hydrodynamic moments were made for wave steepnesses of 0.04 and 0.10 and are included in Figs. 51-54 at the far right of each figure.

## DISCUSSION

### A. Trends of Bending Moment with Wave Steepness

#### 1. Detailed Discussion of Figures 19 to 34.

It is thought to be important to keep in mind the fact that the smooth curves plotted in Figs. 19 to 34 do not represent the variation of one smooth, easily measurable experimental quantity with another. They represent the end product in a data reduction process in which about 20,000 numerical measurements from approximately 400 oscillograph records were compressed into 16 charts. Each line plotted is a least squares fit of an equation to a number of test spots. Each test spot is the average of 5 to 20 maximum sagging (or hogging) moments measured from a time history and plotted against an average wave steepness also measured from a time history.

Ref. 5 contains many references to probable distortion of the time histories of bending moments by relatively long duration impacts, and it was worthwhile to examine, at the source, the faired lines plotted in Figs. 19-34 with respect to how reasonable a fit to the test spots was attained in each case and to note under what circumstances the above-mentioned quasi-impacts were recorded. The results of such an examination follow:

#### a) Figures 19 to 22, Head Seas, Forward Speed

It was noted in the Remarks on the test data which resulted in the faired curves of Fig. 19 (Mariner, parent), that the bending moment traces for 1.0 to 1.50L waves appeared to be distorted and accentuated in the sagging direction by a possible impact forward. An examination of the fit of the curves to the data points indicated that the faired lines are quite good representations of the data. This indicates that if the sagging moment is distorted by a quasi-impact, it is distorted gradually as wave height is increased. (There appears to be no sudden transition between non-impact and impact.) The fit of the hogging data points by the faired curves shown in Fig. 19 is also good in that omission of any point not conforming to the fitted line would not materially change the trend.

Figure 20 shows data obtained for the same conditions as in Fig. 19 but for the Mariner with Cargo Amidship model. Examination of the original data shows that no obvious influence on the bending traces due to impact phenomena were apparent, and in all cases the fit of the faired lines to the data is reasonable.

Figure 21 shows results for the Mariner with Cargo At Ends model. This particular model was visually the worst behaving of all models tested. Examination of the bending moment traces indicate large quasi-impact effects. Notes in Ref. 5 indicate that some significant distortion in the sagging traces was attributable to impact in all wave lengths except 0.75L. As for the Parent Mariner, the fit to the test points for sagging moment was good, thus indicating a gradual distortion with increasing wave steepness. Notations are made for this model that heavy housefront impacts were suspected although no direct evidence could be displayed. Heavy house-front impacts could possibly account for the trend of the hogging moment in the 1.75L wave. This particular curve is the only really unreasonable looking curve of all those that were fitted. However, the fit with the data is quite good and the trouble is with the data itself. The reasons for the behavior of this data are not understood. Because the magnitudes of the hogging moments are lower in this case, than in some other wave lengths, the matter was not pursued. In general, the scatter of the data points about the faired lines for hog for this model was greater than the preceding two models in this speed case, and this is taken as a reasonable indication that there were housefronts impacts, which would tend to reduce or make the average maximum hogging moment erratic. The character of the bending moment traces for this model at this speed is similar to the character of the traces shown for the same model at zero speed in Fig. 12.

Many of the same comments can be made for Fig. 22 showing the results for the Mariner with Increased Freeboard as were made about Fig. 19 for the Parent Mariner. Suspected distortion of the sagging traces by impacts were noted for this model as for the Parent Mariner and the sagging moment fit of the faired curves is considered to be good. The fit of the faired lines to the hogging data points for Fig. 22 is considered good except for those in a wavelength of 1.25L. The discrepancy in this case however is not so great that omission of the one or two points which show the most deviation would materially change the trend of the curve.

To summarize and conclude the comments on this speed-heading case:

- (1) Few really poor fits to the test points were found.
- (2) The data for this speed case is pervaded by cases of quasi-impact.
- (3) The existence of quasi-impact appears to have some effect on the appearance of the families of curves defining the moments for various wave lengths for each model as a function of wave steepness. The one model of the four where no quasi-impact is suspected is the only one where the lines indicating the trend of moment with wave steepness look alike and form a clean pattern (Fig. 20).
- (4) When quasi-impact was suspected, it apparently grew more severe gradually as wave steepness was increased.

b) Figures 23 to 26, Head Seas, Zero Speed

The faired lines represent the data reasonably well in all cases in Fig. 23 which is for the Parent Mariner. No quasi-impact was noted.

In Fig. 24 for the Mariner with Cargo Amidships, all of the faired curves represent test points quite well except for the one for sagging moments in 1.25L waves.

However, omission of either of the two points which do not coincide with the faired line in this case would not materially alter the trend or the magnitude. Similar lack of fit is seen in the hogging moment for the 1.75L wave. Again omission of either of the two points which do not coincide with the fitted line would not materially change the trend. No quasi-impacts were noted.

The bending moment traces which form the source of the data for Fig. 25 (Mariner with Cargo At Ends) show evidence of some impacts in this speed condition. This was the only model with obvious quasi-impacts at zero speed. These impacts are thought to affect the sagging moments and it can be seen that the average trend of sagging moments with wave steepness in this model tends to be more concave upward than the trends of either the Mariner Parent model or the Mariner with Cargo Amidships model (Figs. 23, 24). All the fitted curves are good representations of the test data except for those in the 1.0L wave length. However, none of the deviations shown in that case appear to be too serious.

Figure 26 for the Mariner with Increased Freeboard shows much the same type of trends as for the Mariner Parent at the same speed and heading. The faired lines in all cases reasonably well represent the test data.

To summarize the comments on this speed-heading case:

- (1) Few poor fits to the test points were found.
  - (2) Except for the case of the Mariner with Cargo at Ends, no quasi-impacts were noted. In this case, distortion of the sagging trace was found.
- c) Figures 27 to 30, Head Seas, Drifting

Figures 27 through 30 present data for the four models drifting astern. Results in all these plots are characterized by relatively straighter trends of bending moment with wave steepness than were observed in the head seas zero speed case. The fitted lines in Fig. 27-30 all well represent the data points with two exceptions. One or two points deviate from the fitted lines for the sagging moments in 1.25L and 1.50L waves plotted in Fig. 29 (Mariner with Cargo at Ends model). Omission of these points from the fit would not materially change the trends of the curves, however. The other exception occurs in the sagging moments in 1.50L waves in Fig. 30 for the Mariner with Increased Freeboard. In this case, two points deviate from the faired line and it is possible that omission of these two points would alter the trend shown in Fig. 30 to a more or less straight line. No quasi-impacts were noted in this speed case.

- d) Figures 31 to 34, Following Seas, Forward Speed

Figures 31 through 34 show the faired moments for the four models in following seas at forward speed. The fit of the faired lines to the data points in all of these four figures is not generally as good as that of the head sea cases. Because of the length of test run, instead of 15 or 20 cycles to average as was the case in the forward speed situations, the number of cycles analyzed in the following sea case was 2 to 5. This probably led to a greater scatter of data in this case than in the head sea cases. No quasi-impacts were noted in this case.

## 2. The Absolute Bending Moment Scales and Standard Static Calculations

As a consequence of the method of changing weight distributions from that of the Parent to the models with Cargo Amidships and at Ends, a wide difference in still water bending moments was built into the models. The absolute moment scale in

Figs. 19, 23, 27 and 31 for the Mariner at various speeds and headings show that the controlling design moment would be hogging, as would be the case based on static calculations. The still water moments are so high for the Mariner with Cargo Amidship (Figs. 20, 24, 28, 32) that all the measured moments in extreme seas are sagging moments. Similarly, all the measured moments for the Mariner with Cargo at Ends (Figs. 21, 25, 29, 33) are hogging moments. These remarks tend to point out the extent to which the weight distribution investigation is academic. These variations are and were intended to be extreme.

It is important to note in this connection that the standard static calculations are apparently not valid "yardsticks" for wave moments where highly unusual weight distributions are involved. This point can be illustrated by a comparison of the magnitudes of wave bending moments in Figs. 19 to 21 wherein the static wave moment calculations are identical.

#### B. Trends of Motions Amplitudes with Wave Steepness

Figures 35 through 50 show trends of motions amplitudes with wave steepness. All of the faired curves of motions amplitude for head seas represent the test points quite well except for one case. The case in question is the 1.25L wave for the Mariner with Cargo Amidships at forward speed, (Fig. 36). The scatter of data in this case is considerable. If the most suspect looking point were omitted, the curve would change from convex upward to practically a straight line with about the same ordinate at a wave steepness of 0.1 as shown in Fig. 36. This change would better suit the general trend of the results in the other wave lengths, but there is at present no justification for omitting the point. As for bending moments, the fit of the faired lines to the motions data in the following sea case is not as good as it is for head seas, probably by virtue of the fact that fewer cycles were analyzed to produce each average test point.

It is of interest to compare the general appearance of the figures which represent test results under the same heading and speed conditions. Comparisons of Figs. 35, 36 and 37, 38 which show motions data for four models in head seas at forward speed, shows that the variation of pitching amplitude with wave steepness becomes progressively more non-linear as weight is moved from amidships towards the ends. It is of interest to note that heaving amplitude trends generally appear to be similar for all models. The general appearance of the trends of pitch amplitude and heaving amplitude for the Mariner with Increased Freeboard are about the same as those for the Parent Mariner. The same remarks about the differences in trends of pitching amplitude with wave steepness may be made for the head sea, zero speed case (Figs. 39-42). The trends of motion amplitudes for the head sea-drifting and the following sea-forward speed cases (Figs. 43-50) approximate straight lines with one exception. The exception is in the Mariner with Cargo Amidships in following seas, in the 1.75L and 1.5L wave lengths, (Fig. 48). In both wave cases pronounced convex upward pitch trends are shown. These trends result from test spots which showed considerable scatter about the mean lines and which were derived from quite small numbers of cycles. The number of cycles in the two cases ranged from 2 to 5. It is possible in this case that the results from these two wave lengths should be disregarded.

#### C. Results of the Numerical Classification of Trends with Wave Steepness

Table IV summarizes results of a numerical classification of trends with wave steepness of moments and motions for the weight distribution investigation. Table V summarizes results for the Freeboard investigation. It is noted that zero in the table signifies a relatively straight line variation. The minus sign denotes the beginning of a convex upward trend, two minus signs denote a definite convex upward trend. Insofar as ascertaining maximum physically possible moments, the minus-

minus designation is the most favorable situation. On the other hand, a plus-plus designation means that the moments or motions are concave upward and this is a distinctly bad indication of an upper bound. The asterisks indicate those cases where it was noted that a suspicion of distortion of moment trace by impact was present. The results in the tables for the 1.75L waves were in almost all cases obtained by extrapolating the mean lines somewhat further than was done in the Figs. 19 through 50. This means that there was not enough initial data present in the higher wave steepnesses to justify extending the line to this extent and the classification of trend results must be viewed in this light.

The first six columns of Tables IV and V are the most important to the main objective of this investigation; that is to confirm the existence of an upper bound on bending moments.

The following table summarizes the incidence of the various classification results for hog and sag.

<u>Class</u>	<u>Incidence, % of Total</u>	
	<u>Sag</u>	<u>Hog</u>
++	0	3
+	20	17
0	62	45
-	18	21
--	0	14

It is plain that the preponderance of results centers about class 0, the straight line trend.

As has been noted, a double plus entry denotes a negative answer: no upper bound. This entry occurs twice in the first six columns of Table IV. The first entry is for the hogging moments for Mariner with Cargo at Ends in head seas, forward speed, wave length 1.75L. It was noted in a previous section that the faired line for this case showed an unreasonable trend of hogging moments - the reason being that no hogging moments were indicated for moderately steep waves. Since no actual data was obtained in this wave steepness range, the trend shown must be viewed with skepticism.

The second double-plus entry is for the Mariner with Cargo Amidship in following seas, 1.50L wave length, where the results are characterized by: 1) short test runs, 2) consequently a small number of cycles to analyze, 3) a rather large scatter of the individual measurements which make up the individual test points, and 4) a not exceedingly good representation of the test points by the fitted line. It is believed that the above remarks sufficiently qualify the two trends in question so that they can be omitted from consideration. The double-plus sign does not occur at all in the first six columns of Table V.

These remarks indicate that the only convex upward trend of bending moments with wave steepness which is likely to be encountered is a weak divergence from a straight line.

On the positive side of the question of the existence of an upper bound is the incidence of double negative signs in Tables IV and V - ten cases in all, not counting the repeated Parent Mariner entries in Table V. All of these cases occur in head seas at zero or forward speed for hogging moments. Six of these ten cases occur at high forward speed, the remainder for one model at zero forward speed. It is seen that in order to obtain strong indications of an upper bound on bending

moments for the four models tested, two useful but impractical artifices have been employed. The first is that of an impracticably high forward speed for the steepest waves. The second has been a change in weight distribution so extreme that the resulting still water bending moments exceed the measured wave moments in the highest waves. True, for the case in question (the Mariner with Cargo at Ends at zero speed), the sense of the still water moment is such that a design limit is implied (see Fig. 25) but the magnitude of this design limit significantly exceeds the magnitude of the highest absolute moment measured in the Parent model (Fig. 23), and it is doubtful that redistributing the ship mass toward the ends should result in anything but a higher structural weight.

It appears that where a very strong indication of a limiting trend of bending moments with wave steepness is found, practical considerations of ship operation or design tend to override.

Of the remainder of the entries in the tables, most are zeros which indicate a more or less straight line variation of bending moment with wave steepness. Single minus signs which indicate the beginning of a leveling out trend are the next most frequent symbol. In the case of the single minus sign, the limiting moment would occur at a wave steepness exceeding  $1/9\text{th}$ . It is clear that in order to attain consistent and definite limits on bending moments, wave steepnesses up to the theoretical deep water maximum must be considered and that it is possible that entry into the region of standing waves where greater steepnesses are possible would be required. It is possible that this course of action would be as far away from practicability as the high forward speed case in head seas, since the present range of data ended with wave heights which, scaled to suit a 500 foot ship, were about equivalent to the highest waves reliably reported to have occurred at sea.

It seems reasonable to conclude that within practical merchant type surface ship operational and design limits and within a very wide range of wave steepnesses, no definite limit on bending moments is to be expected as wave steepness increases, and in fact, the moments appear to be grossly proportional to wave steepness over quite a large range of steepness.

If the assumptions are made that 1) the ship would be impossible to control at high speed in extreme following seas, and 2) that the ship could make no more than zero speed in head seas, then from a comparison of the cross plots of Figs. 52 and 53, the ship will be subjected to the same magnitude of bending moments either by just holding its own, or drifting helplessly before the waves. Comparison of the applicable blocks in Tables IV and V shows that nearly straight line variation or a small non-limiting trend of moment with wave steepness occurs for virtually every model in every wave length for one or the other speed case. Thus, since the design must be predicated on the worst case, not even the beginning of a limiting trend may be taken under the above assumptions.

It is of interest to compare the classification of trends of the hydrodynamic sagging moment in Tables IV and V with the measured sagging moments (first and fifth columns). It can be seen that the conversion of the measured sagging moment to the approximate hydrodynamic sagging moment results in trends with wave steepness which are straighter. This is more strongly illustrated for the hydrodynamic hogging moment at forward speed and at the zero speed, where it can be noted that the strong limiting trends shown for the hogging moment at zero speed for the Cargo at Ends model are virtually erased when the moments are corrected to "hydrodynamic."

The conclusion that "hydrodynamic" moments tend to be straighter than measured is very surprising since one would not expect what appears to be an obviously non-linear problem to result in a nearly straight line trend.

#### D. Additional Confirmation of the Results of Section C

The practical basis of these conclusions hinges on trend of the moments measured in the most severe wave lengths. Limiting trends displayed in other wave lengths may have little practical significance. In order to help confirm the conclusions obtained, a fresh start on the analysis was made without benefit of fitted lines or numerical manipulation. Reference 5 was consulted and every test point obtained in any wave condition and at all of the four speeds was plotted on a single chart for each model. The only differentiation between points which was made was between those for the impractical head-sea forward-speed case (solid circles) and those for all other speeds (open circles).

The results are shown in Figs. 63 to 66. Envelopes to the scatter of points were drawn up to a wave steepness of 0.10, excluding the points for the head-sea forward-speed case. The envelopes were terminated at  $h/\lambda = 0.10$  because the long wave lengths which contribute many of the highest moments, are not well represented beyond this point. It can be seen that the envelopes of all moments measured at practical speeds in all models imply no limit at a wave steepness less than  $1/9$  and most imply no limit until the theoretical limit of stability ( $1/7$ ).

It is interesting to compare these results with those of Ref. 9. The experimental work of Ref. 9 was quite different from that reported herein in that it dealt with irregular model seas. It was similar in that the severity of the irregular waves of Ref. 9 was comparable to the severity of the regular waves of this study. As in the present results, those of Ref. 9 imply that midship bending moment ranges are proportional to wave steepness over a very large range of steepness. (No distinction could be made in Ref. 9 between hogging and sagging moment trends.) It is therefore considered likely that the trends of bending moment with wave steepness shown herein approximate those expected for significant bending moment amplitudes in random seas of increasing severity.

#### E. Maximum Moments in Waves of Constant Height

If, instead of assuming that waves of limiting steepness in any length are possible or probable at sea, one assumes that probable waves will be no higher than some constant value it may be possible to develop a reasonable maximum bending moment. This is not a physical upper limit, but a limit dictated by a maximum wave height. Figures 57, 58 and 59 show one such development for a constant wave height of 10% of the ship length. It can be seen in all these figures, in contrast to the cross-plots for constant wave steepness, that bending moments in extreme waves tend to reach maximum values in wave lengths between 1 and  $1-1/4$  ship lengths. This is in agreement with results from bending moment tests with ship models in moderate regular waves of constant height. Figure 60 is a plot of the maximum moments measured in waves of 10% the model length, plotted on a base of speed. Here again, it is obvious that there is not much choice between running the ship into head seas, letting the ship drift in head extreme seas or running at high speed in following seas. No large reduction in extreme bending moments appears to be possible.

#### F. Comparisons Between Models

While not directly in line with the main objective of the investigation which was to define the existence or non-existence of an upper physical limit of bending moments, a comparison between the model variations tested is instructive and the cross plots in Figs. 51 through 54 can be advantageously used for this purpose.

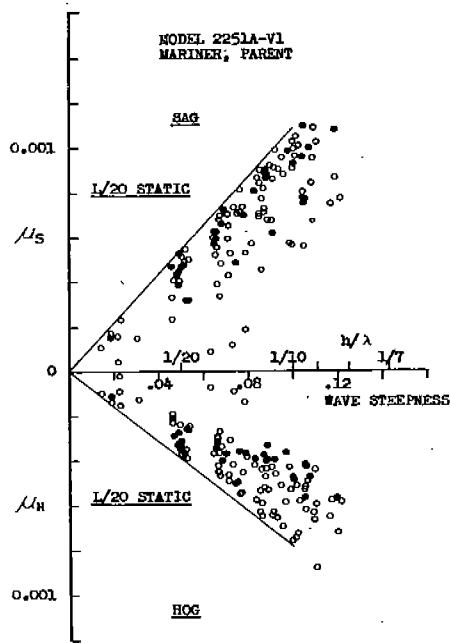


FIG. 63.

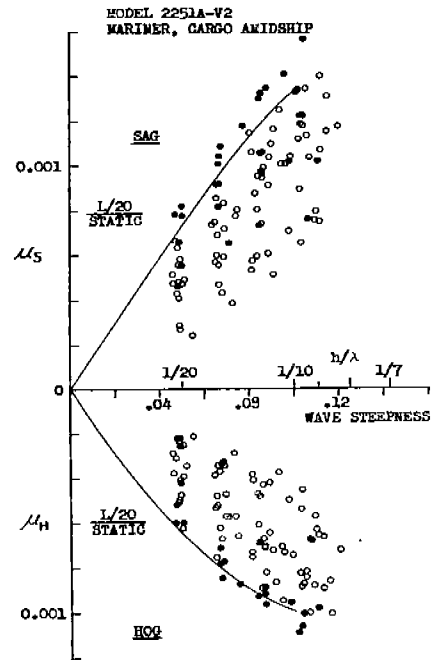


FIG. 64.

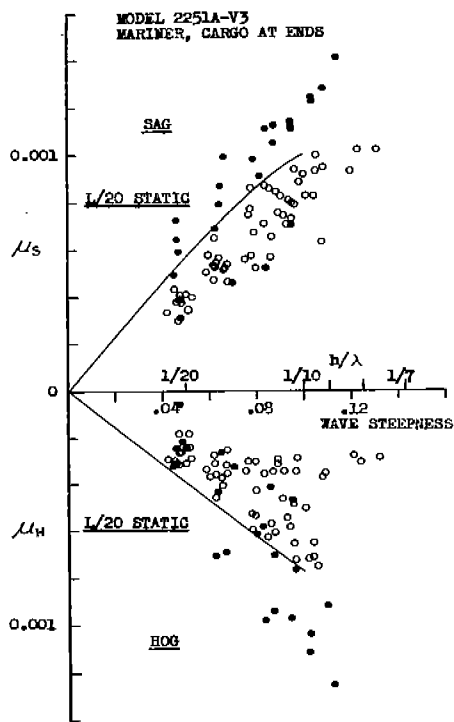


FIG. 65.

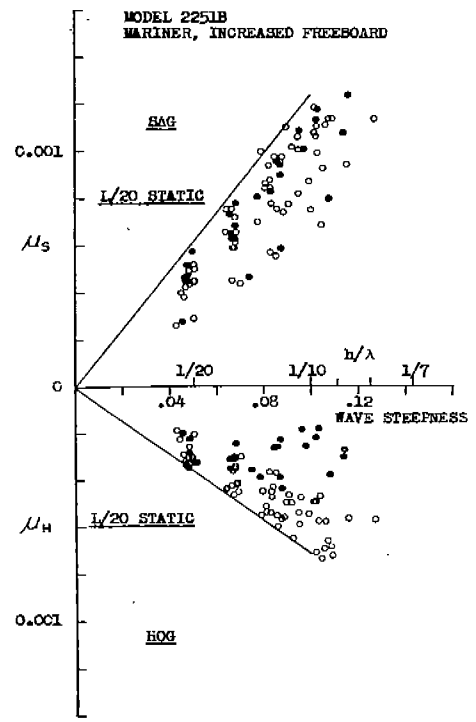


FIG. 66.

FIG. 63-66. MEASURED BENDING MOMENT DATA, ALL WAVE LENGTHS AND SPEEDS.

## 1) Weight Distribution Investigation

It is advantageous to start the discussion of the differences between models within this investigation with Fig. 52 where data for head seas at zero speed is presented. It can be seen that measured bending moments for the Mariner with Cargo at Ends appear to be lowest. Next in magnitude are bending moments of the Parent Mariner and highest are those for the Mariner with Cargo Amidships. Quite sizeable differences are shown in the bending moments at a wave steepness of both .10 and .04. The exception to this progression occurs in the sagging moment for the Mariner with Cargo at Ends at a wave steepness of 0.1. It should be remembered, however, that the sagging moments for the Mariner with Cargo at Ends at this speed were the only ones obviously affected by a quasi-impact of the bow and this may account for the difference in progression. It is of interest to compare the crossplots of measured moments with those for the approximate hydrodynamic moment (far right of the figure). While the "hydrodynamic" moments are higher than the measured, it can be seen that the percentage differences between models tend to disappear.

An examination of the two succeeding crossplots for head seas, drifting and for following seas, high speed show that the differences in measured bending moment between models are less pronounced but usually in the same progression as for zero speed and that the differences between the approximate hydrodynamic moments for the three models are generally smaller, percentage-wise, than those between the measured moments. The exception to this trend is shown in Fig. 51 for head seas, forward speed. It can be seen that the wide differences between the moments observed in the Mariner, Parent and in the Mariner with Cargo Amidship disappear when the moments are converted to hydrodynamic moments. However, the same does not hold true for the moments observed for the Mariner with Cargo at Ends. If one assumes that the hydrodynamic moment as derived is correct in detail, then the difference between the crossplots of hydrodynamic moment for the parent model and those for the Mariner with Cargo at Ends represents the difference in integrated water pressures and this difference might be attributed to quasi-impacts, known to be more severe for this model than for the other models.

The conclusion to be drawn from this comparison between models is that the primary cause of difference in bending moments between the three models in the weight distribution investigation is the difference in mass moments; that is, differences in centers of longitudinal centers of gravity of each half of each model. It was found in a previous section that the predominant term in the calculation of the average moment due to accelerations involved the product of heave amplitude and average mass moments about amidship. Since the heave amplitudes are nearly the same in this case for the three models, the primary cause of the differences in moment is attributed to differences in mass moments.

## 2) Freeboard Investigation

Inspection of the crossplots in Fig. 51 through 54 show that the measured bending moments of the Mariner with Increased Freeboard are generally quite close to those of the Parent Mariner. The main exception is in the sagging moment in extreme waves where it was expected that the increased buoyancy of the model would generate higher vertical forces on the bow when the bow was submerged. From the preceding discussion of the importance of weight moments it would not appear that there would be any differences in the comparison of "hydrodynamic" moments for the Parent Mariner model and the Mariner with Increased Freeboard. This was not the case. In most cases the differences between the "hydrodynamic" moments for the Parent model and the Mariner with Increased Freeboard tended to be smaller than the corresponding differences in measured moment. Since there is no difference in the mass moments about

amidships for the two models, the explanation must lay in different heaving and pitching motions, and this was generally found to be the case. In the head sea forward speed and the head sea zero speed cases, there is a residual difference in hydrodynamic sagging moments between the Mariner with Increased Freeboard and the Parent Mariner. This occurs in the extreme waves of .1 steepness and probably reflects the increase in reserve buoyancy of the high freeboard model.

#### CONCLUSIONS

1. It appears on the basis of these studies that design wave bending moments for the Mariner type ship are essentially proportional to the wave heights which actually may be encountered.
2. The present study, by establishing more firmly the grossly linear dependence of moments on wave heights over a considerable range of wave severity, has strengthened the case for determining design moments on the basis of statistical analyses of sea waves and/or the resulting moments.
3. It is concluded that, within practical operational and design limits for the Mariner type ship, no significant limit on midship wave bending moments in head or following waves is to be expected as wave steepness is increased up to a value of about  $1/9$ .

#### RECOMMENDATIONS

The present study involved itself only with midship bending moments for reasons of economy, even though it was known that under certain conditions higher wave bending moments may develop elsewhere along the ship length. It is considered of importance to ascertain if the conclusions of this study also hold for moments all along the length of the ship. If similar conclusions can be drawn for moments elsewhere along the length of the ship, no further development of this type of experiment would be recommended.

#### ACKNOWLEDGEMENTS

The author wishes to acknowledge with thanks the excellent guidance and stimulus extended by the Project Advisory Committee headed by Mr. M. Forrest. The assistance rendered by a large number of members of the Davidson Laboratory staff is also acknowledged with thanks. Prominent among the many contributors were Messrs. E. Numata, S. Chuang, Y. Chey, R. Clapp and W. Klosinski of the Ship Research Division, Miss A. Von Zumbusch and Mr. F. Behrens of the Computing Department, Mr. H. Deroian of the Photo Department, and Mrs. M. Brovarone, Secretary.

Much of the data reduction was done on the IBM 1620 Computer now being operated as part of the Computer Center of the Stevens Institute of Technology, which is partly supported by the National Science Foundation.

#### REFERENCES

1. Lewis, E.V. and Gerard, G.: "A Long-Range Research Program in Ship Structural Design," Ship Structure Committee, Serial SSC-124, November 1959.
2. Dalzell, John F.: "An Investigation of Midship Bending Moments Experienced in Extreme Regular Waves by Models of a Tanker and a Destroyer," O.T.S. Report PB 181509.

3. McGoldrick, R.T. and Russo, V.L.: "Hull Vibration Investigation on S.S. GOPHER MARINER," SNAME Transactions, Vol. 63, 1955.
4. Solodovnikov, V.V.: "Introduction to the Statistical Dynamics of Automatic Control Systems," Dover Publications, New York, 1960.
5. Dalzell, John F.: "An Investigation of Midship Bending Moments Experienced in Extreme Regular Waves by Models of the Mariner Type Ship and Three Variants. DL Report 926, November 1962.
6. DeDoes, J.C.: "Experimental Determination of Bending Moments for Three Models of Different Fullness in Regular Waves," Report 36S, Netherlands Research Center, T.N.O. for Shipbuilding and Navigation, April 1960.
7. Dalzell, J.F.: "Effect of Speed and Fullness on Hull Bending Moments in Waves," DL Report 707, February 1959.
8. Report of the Committee on Wave Loads, Proceedings of the International Ship Structures Congress, Glasgow, 1961.
9. Dalzell, John F.: "Some Further Experiments on the Application of Linear Superposition Techniques to the Responses of a Destroyer Model in Extreme Irregular Long-Crested Head Seas," DL Report 918, September 1962.

#### NOMENCLATURE

Arg:	= Argument
$A_2$	= Coefficient in equation of $\bar{M}_{FA}$
a,b,N	= Coefficients
B	= Maximum Model Beam
C	= Non-Dimensionalized Bending Moment (Bending Moment/ $\rho g L^2 B h$ )
$C_2$	= Coefficient in equation of $\bar{M}_{FA}$
$C_B$	= Block Coefficient
$C_R$	= Midsection Coefficient
d	= Duration of Response to Half Sine Pulse, at Midheight
D	= Duration of Half Sine Pulse
E	= Maximum Response of Measuring System to Half Sine Pulse
g	= Acceleration due gravity
H	= Draft
h	= Wave Height
$h/\lambda$	= Wave Steepness
$K_o$	= Longitudinal Gyradius
L	= Model length on 20 stations
LBP	= Length between Perpendiculars
LCG	= Longitudinal Center of Gravity
M	= Bending Moment, General

$\bar{M}_{FA}$	= Average Midship Bending Moment Due to Acceleration of Model Mass
$\bar{M}_{RE}$	= Part of $\bar{M}_{FA}$ in Phase with Measured Bending Moments
Mod:	= Modulus
R	= Model Resistance in Waves
rms	= Root-mean Square
t	= Time
V	= Model Speed
VCG	= Vertical center of gravity
Y	= General Response
$Z_o$	= Heaving Amplitude
$2Z_o/L$	= Non-Dimensional Heave Double Amplitude
$Z_{LCG}$	= Heave at LCG
$Z_{pp}$	= Heave at Pitchpivot
$\alpha, \beta, \gamma$	= Quantity Derived in the Numerical Classification of Trends
$\Delta$	= Model Displacement
$\delta$	= Heave Phase Angle
$e$	= Pitch Phase Angle
$\theta$	= Pitch Angle
$2\theta_o$	= Pitch double Amplitude
$\lambda$	= Wave Length
$\lambda/L$	= Wave Length to Model Length Ratio
$\mu_H$	= Hogging Moment Coefficient (hogging moment/ $\rho g L^3 B$ )
$\mu_S$	= Sagging Moment Coefficient (sagging moment/ $\rho g L^3 B$ )
$\mu_H^i$	= Approximate Hydrodynamic Hogging Moment ( $\mu_H - \bar{M}_{RE}$ )
$\mu_S^i$	= Approximate Hydrodynamic Sagging Moment ( $\mu_S - \bar{M}_{RE}$ )
$\mu_{HA}$	= Absolute Hogging Moment - Non-dimensional
$\mu_{HS}$	= Absolute Sagging Moment - Non-dimensional
$\rho$	= Mass Density of Water
$\omega_e$	= Frequency of Wave Encounter

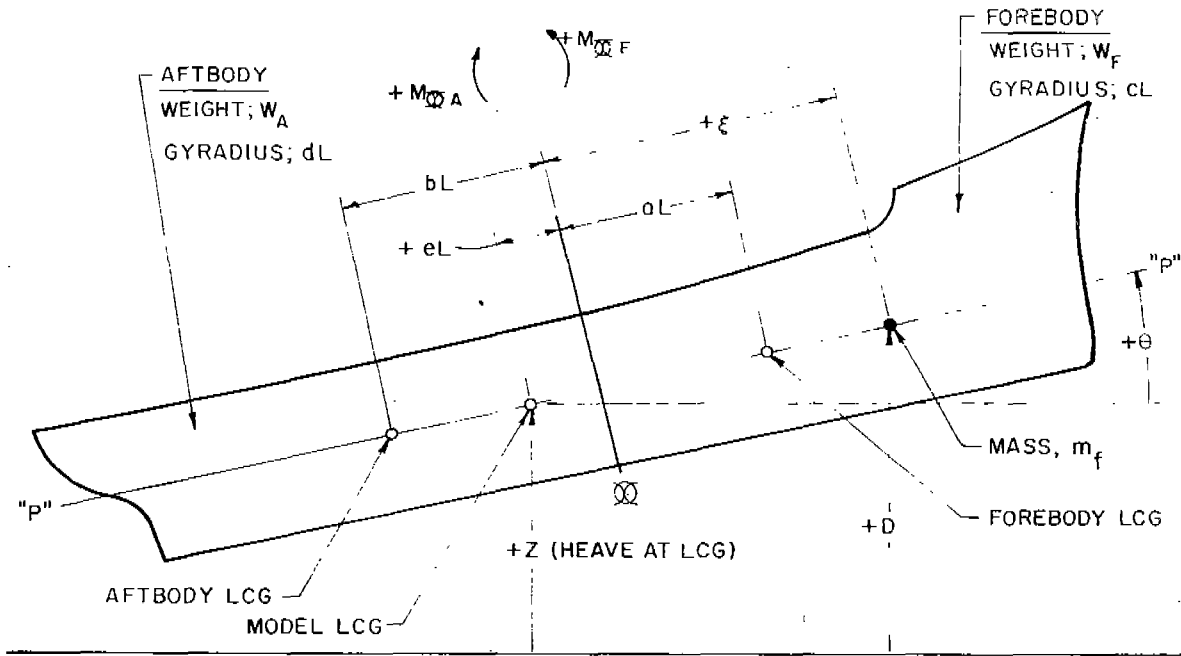


FIG. 67. NOTATION FOR DERIVATION IN APPENDIX.

APPENDIX

Approximation to the Component of Midship Bending Moment  
Due to the Pitch and Heave Accelerations Imposed on the Model.

A sketch showing the necessary notation is presented in Fig. 67. The model consists of two rigid bodies connected by a spring amidships. Since the actual models are relatively long and slender it is assumed that negligible error will result if all weight is assumed concentrated along a line in the center plane, parallel to the keel, and passing through the vertical center of gravity of the model. (Line  $\bar{P}\bar{P}$ , Fig. 67) pitching angle is assumed to be  $-15^\circ$  or less and thus the vertical acceleration at a point on the line  $\bar{P}\bar{P}$  closely approximates the normal acceleration.

Under these assumptions the midship bending moment caused by the normal acceleration of an elemental mass,  $m_f$ , (see Fig. 67) is nearly:

$$\delta M_{BF} = - \epsilon m_f \ddot{D} \quad (1)$$

Again under the assumption of relatively small pitch angles:

$$D = Z + (\epsilon + eL)\theta \quad (2)$$

and:

$$\ddot{D} = \ddot{Z} + (\xi + eL)\ddot{\theta} \quad (3)$$

Substituting:

$$\delta M_{BF} = - (\ddot{Z} + \ddot{\theta} eL) m_f \cdot \xi - \ddot{\theta} m_f \xi^2 \quad (4)$$

Summing the contributions from all the elements of mass in the forebody:

$$M_{\text{BF}} = - (\ddot{Z} + \ddot{\theta} eL) \sum_0^{L/2} m_{\xi} \xi - \ddot{\theta} \sum_0^{L/2} m_{\xi} \xi^2$$

$$= - (\ddot{Z} + \ddot{\theta} eL) \frac{W_F}{g} aL - \ddot{\theta} \frac{W_F}{g} (a^2 L^2 + c^2 L^2) \quad (5)$$

Similarly for the aft body with attention to the sign conventions shown in Fig. 67:

$$M_{\text{BA}} = - (\ddot{Z} + \ddot{\theta} eL) \frac{W_A}{g} bL + \ddot{\theta} \frac{W_A}{g} (b^2 L^2 + d^2 L^2) \quad (6)$$

Rearranging:

$$M_{\text{BF}} = - A_1 \left( \frac{2\ddot{Z}}{L} \right) - C_1 (2\ddot{\theta}) \quad (7)$$

$$M_{\text{BA}} = - B_1 \left( \frac{2\ddot{Z}}{L} \right) - D_1 (2\ddot{\theta}) \quad (8)$$

where:

$2\ddot{\theta}$  is in degrees/sec<sup>2</sup>

$$A_1 = + aW_F L^2/2g \quad \text{Ft Lb Sec}^2$$

$$B_1 = + bW_A L^2/2g \quad \text{"}$$

$$C_1 = (ae + a^2 + c^2)W_F \cdot L^2 \pi/360g \quad \frac{\text{Ft Lb Sec}^2}{\text{Degree}}$$

$$D_1 = (be + b^2 + d^2)W_A \cdot L^2 \pi/360g \quad \text{"}$$

Assuming harmonic motions

$$\ddot{Z} = - \omega_e^2 Z_o \cos (\omega_e t - \delta) \quad (9)$$

$$\ddot{\theta} = - \omega_e^2 \theta_o \cos (\omega_e t - \epsilon) \quad (10)$$

Where  $\delta$  and  $\epsilon$  are phase lags of maximum upward motion after maximum sagging moment and  $\omega_e$  is the wave encounter frequency.

Substituting (9) and (10) into (7) and (8), expanding and re-arranging:

$$M_{\text{BF}} = \left[ A_1 \omega_e^2 \left( \frac{2Z_o}{L} \right) \cos \delta + C_1 \omega_e^2 (2\theta_o) \cos \epsilon \right] \cos \omega_e t$$

$$+ \left[ A_1 \omega_e^2 \left( \frac{2Z_o}{L} \right) \sin \delta + C_1 \omega_e^2 (2\theta_o) \sin \epsilon \right] \sin \omega_e t \quad (11)$$

$$M_{QA} = \left[ B_1 \omega_e^2 \left( \frac{2Z_o}{L} \right) \cos \delta + D_1 \omega_e^2 (2\theta_o) \cos \epsilon \right] \cos \omega_e t$$

$$+ \left[ B_1 \omega_e^2 \left( \frac{2Z_o}{L} \right) \sin \delta + D_1 \omega_e^2 (2\theta_o) \sin \epsilon \right] \sin \omega_e t \quad (12)$$

(2θ<sub>o</sub> in Degrees)

Since ships do not generally have their LCG at amidship A<sub>1</sub> and B<sub>1</sub> are not usually equal. C<sub>1</sub> and D<sub>1</sub> are usually unequal for about the same reason. Thus

$$M_{QF} \neq M_{QA} \text{ (usually)}$$

The bending moments from all sources forward of amidships must equal those from sources aft of amidships.

If: H<sub>QF</sub> and H<sub>QA</sub> denote hydrodynamic bending moments:

And: M<sub>Q</sub> = Total midship moment

$$M_Q = M_{QF} + H_{QF} = M_{QA} + H_{QA}$$

$$= \frac{M_{QF} + M_{QA}}{2} + \frac{H_{QF} + H_{QA}}{2} \quad (13)$$

In order to simplify the analysis, the average of the forward and aft moments due to acceleration of model mass was calculated:

$$\bar{M}_{FA} = \left[ A_2 \omega_e^2 \left( \frac{2Z_o}{L} \cos \delta \right) + C_2 \omega_e^2 (2\theta_o \cos \epsilon) \right] \cos \omega_e t$$

$$+ \left[ A_2 \omega_e^2 \left( \frac{2Z_o}{L} \sin \delta \right) + C_2 \omega_e^2 (2\theta_o \sin \epsilon) \right] \sin \omega_e t \quad (14)$$

where:

$$A_2 = (aW_F + bW_A) L^2 / 4g$$

$$C_2 = \left[ (ae + a^2 + c^2)W_F + (be - b^2 - d^2)W_A \right] \cdot L^2 \pi / 720g$$

(2θ<sub>o</sub> in Degrees)

SHIP HULL RESEARCH COMMITTEE  
Division of Engineering & Industrial Research  
National Academy of Sciences-National Research Council

Chairman:

RADM A. G. Mumma, USN (Ret.)  
Vice President  
Worthington Corporation

Members:

Mr. Hollinshead de Luce  
Assistant to Vice President  
Bethlehem Steel Co. Shipbuilding Div.

Professor J. Harvey Evans  
Professor of Naval Architecture  
Massachusetts Institute of Technology

Mr. M. G. Forrest  
Vice President - Naval Architecture  
Gibbs & Cox, Inc.

Mr. James Goodrich  
Vice President and General Manager  
Todd Shipyards, Los Angeles Div.

Professor N. J. Hoff  
Head, Dept. of Aeronautics & Astronautics  
Stanford University

Mr. M. W. Lightner  
Vice President, Applied Research  
U. S. Steel Corporation

Dr. J. R. Low, Jr.  
Metallurgy & Ceramics Research Dept.  
General Electric Research Laboratory

Arthur R. Lytle  
Director

R. W. Rumke  
Executive Secretary